quaternary

MDPI

Article

Treponematosis Evidence in Human Skeletons of 15th–19th Centuries, Discovered in Iași City (Eastern Romania)

Vasilica-Monica Groza [1], Mariana Popovici [1], Anca-Narcisa Neagu [2], Luminița Bejenaru [1,2,*] and Ozana-Maria Ciorpac-Petraru [2,*]

[1] "Olga Necrasov" Center of Anthropological and Biomedical Research, Iasi Branch of Romanian Academy, 700481 Iaşi, Romania; groza.monica@acadiasi.ro (V.-M.G.); popovici.mariana@acadiasi.ro (M.P.)
[2] Faculty of Biology, "Alexandru Ioan Cuza" University of Iaşi, 700505 Iaşi, Romania; aneagu@uaic.ro
* Correspondence: lumib@uaic.ro (L.B.); ozana.ciorpac@uaic.ro (O.-M.C.-P.)

Abstract

Syphilis, caused by the bacterium Treponema pallidum, has a complex evolutionary history, most likely being transferred from the Americas to Europe after the 15th century and subsequently spreading widely through sexual transmission. This work is one of the few studies on the skeletal evidence of probable treponematosis in archaeological populations discovered on the Romanian territory, providing data to better understand the disease history. Pathological lesions identified in three human skeletons of the 15th–19th centuries are described, and a diagnosis of treponematosis is performed. The three analyzed skeletons were discovered during the archaeological excavations in the necropolis of the Roman-Catholic Cathedral in Iasi City (Romania). The investigated skeletons belonged to individuals aged 30–40 years old (two females and one male). Somatoscopic, radiographic, tomographic, and microscopic examinations were used for the differential diagnosis. The results of multiple investigation methods support the diagnosis of probable treponematosis in all three skeletons, showing different stages of caries sicca in skull bones, cortical thickening, and new periosteal bone formation in postcranial bones.

Keywords: osteopathology; macroscopy; microscopy; Eastern Romania; 15th–19th centuries

1. Introduction

Treponematosis or treponemal disease is a chronic infection caused by spirochete bacteria of *Treponema* genus [1]. There are four syndromes of the disease, classified according to clinical manifestation: pinta caused by *T. carateum*; yaws caused by *T. pallidum pertenue*; bejel or endemic syphilis caused by *T. pallidum endemicum*; and acquired syphilis associated with *T. pallidum pallidum* [2–6]. The relationship of pinta to the infections caused by *Treponema pallidum* subspecies, however, is little known. Treponematosis has long been the topic of speculation concerning its origin, past distribution, clinical presentation, nature of the causative agents, and epidemiology of the currently recognized clinical phenotypes [7,8].

In treponematosis, skeletal lesions occur in only the secondary and tertiary stages of disease [9,10]. Age of onset (primary infection) is typically less than 15 years of age for yaws, between ages 2 and 15 years for bejel, and over 15 years for syphilis [11].

Treponematosis is thought to have originated during the Paleolithic period as a disease transmitted by skin-to-skin contact in the hot and humid climate of sub-Saharan Africa [12]. The infection would have accompanied hunter–gatherers in their migrations around the world [13]. Although there are many studies on treponematosis [14–16], its origin and

Check for updates

Academic Editor: Miriam Belmaker

Received: 20 February 2026
Revised: 5 April 2026
Accepted: 30 April 2026
Published: 12 May 2026

Copyright: © 2026 by the authors. Licensee MDPI, Basel, Switzerland. This article is an open access article distributed under the terms and conditions of the Creative Commons Attribution (CC BY) license.

spread are still controversial—it is not well known if it accompanied the *Homo* evolution during more than a million years or it emerged only after Columbus's return to Europe [17].

Furthermore, evidence of *Treponema pallidum* infection in nonhuman primates suggests the existence of potential animal reservoirs and that cross-species transmission may also have contributed to the spread of treponematoses [18,19]. In his substantial study of treponematosis in dry bones, Hackett [20] described the most common destructive and proliferative lesions and identified a series of progressive cranial lesions referred to as the *caries sicca*. The skeletal lesions caused by treponematosis result from both osteoblastic and osteoclastic activity and can be classified as gummatous (soft, tumor-like, granulomatous lesions that cause destructive inflammatory tissue damage, occurring in the tertiary stage) and non-gummatous (inflammatory bone lesions like periostitis, osteitis, or osteomyelitis, often seen in the secondary stage). Gummatous lesions are mainly lytic and characterize the advanced disease [21,22]; they can be found especially on the skull but also on long bones. In severe cases of treponematosis, lesions called *caries sicca* are reported on the cranium [21]. Non-gummatous lesions appear in the form of periostitis and osteitis [21–23], affecting bones in the postcranial skeleton [21,22]. The significant periosteal deposition on the anterior shaft of the tibia is described as a "sabre shin" deformity, and it is a defining characteristic of treponematosis [21–23]. Other non-gummatous reactions involve the narrowing of the medullary cavity in long bones by increased cortical thickening and trabecular bone growth [21].

The treponematoses in skeletal remains have been intensely debated, and they continue to be a contentious issue in science [24]. Acquired syphilis is conceivably the most well-known of the treponematoses, especially in the modern Western world. This has an unlimited global distribution, unlike its counterparts [21], and has no climatic requirements [3,23]. Questions about the time period in which syphilis developed and where the source of this infection came from are still debated [25]. Regarding the origin and spread of acquired syphilis throughout the world, three hypotheses currently exist: the Columbian, the pre-Columbian and the Unitarian [13,23]. According to them, syphilis originated either in the New World [26–28] or in the Old World [29–31], or respectively it was present in both regions, but it evolved in different geographical and sociological environments [3,32].

Acquired syphilis is called the Great Imitator because both its clinical pathogenesis and skeletal alterations are quite similar to other diseases (e.g., tuberculosis, hematogenous osteomyelitis, and Paget's disease). This is especially true when a skeleton is partially available for observation [3].

According to clinical data, approximately 20–50% of untreated cases of acquired syphilis progress to the tertiary stage [21], and only 10–12% of individuals with syphilis exhibit bone changes [6,33]. These data could explain the rarity of such affected skeletons discovered in archaeological contexts.

Immunological and genetic studies indicated that the same spirochete species, *Treponema pallidum*, causes yaws, bejel and syphilis [13,34]. Conversely, ulterior molecular research has identified distinctions in the treponemal DNA [35]. The study by Gray et al. [36] shows that the sequences of the subspecies *Treponema pallidum pallidum* have too many variations to support the hypothesis of the evolution of acquired syphilis in the last 500 years. Opposite to this, another study [37] indicates that acquired syphilis appeared recently in human history (~500 years ago) from a New World progenitor related to yaws [38].

Although initial expectations were dampened by indications that treponemal DNA would either not preserve [39] or would be recovered only in rare cases [40], the number of historic individuals yielding treponemal DNA at the genome level is increasing [41–43]. Genetic studies agree in their conclusion that yaws is much younger than previously thought [42,43] and further indicate that both yaws and syphilis underwent a substantial

increase in genetic diversity approximately 500 years ago [42–44]. The small number of ancient genomes yielded, however, is insufficient to answer the questions related to the global distribution of these pathogens before 1492, especially those controversies surrounding the origin of syphilis [45].

This paper presents new evidence of possible treponematosis discovered in archaeological populations from Romania. In our study, we describe three skeletons with multiple pathological lesions, and we propose a differential diagnosis. The morphology and structure of the identified lesions indicate acquired syphilis. A preliminary macroscopic paleopathological analysis of one skeleton (R26) has already been published [46].

Although several cases of syphilis have been reported in archaeological populations of Europe [6,47–54], in Romania, the closest chronological analogy is only that of the case identified in the necropolis of the 16th–19th centuries from the Saint Sava Church in Bucharest. There, the pathological lesions found on seven skeletons are consistent with treponematosis [55]. The distribution and morphology of the lesions are significant of treponematosis, which makes this the first case in an archaeological population reported for Romania.

2. Historical Context

The urban settlement of Iaşi (Iaşi County, Romania) (Figure 1) is proven by archaeological discoveries since the end of the 14th century and the beginning of the 15th century [56].

Iasi was the former capital city of Medieval Moldavia (1564–1859), and it was marked by quasi-permanent calamities, often suffering from repeated Tatar, Ottoman, and Polish invasions [57]. During the medieval and postmedieval times, the sanitary deficiencies in this area led to many diseases and implicitly to an increase in the number of deaths recorded [56].

The history of the Catholic community in Iaşi began at the end of the 14th century, and it is closely related to the foundation of Medieval Moldova and to the development of its towns [58]. The settlement of Iaşi was located at the juncture of several important geographical units (Central Moldavian Plateau, Suceava Plateau and Moldavian Plain) at the crossroads between significant commercial routes connecting the Baltic Sea to the eastern basin of the Mediterranean and Central Europe to Tatar lands. These geographic circumstances favored the economic development of the city and the settling down of a heterogeneous population [59]. Many ethnic groups with different and complementary cultural values inhabited the urban agglomeration of Iasi alongside the local population [60]. In Iaşi, Greeks, Serbs, Bulgarians and Albanians were established as merchants and assimilated in time due to the confessional fit with the majority population [61]. Therefore, the merchants could have provided a transmission way for the treponematosis.

The Catholic population of Iaşi city knew a significant diversity over time—Germans, French, Italians, Hungarians and Polish, all rallied under the Catholic Church umbrella [60].

The number of Catholics in Iaşi, originating from all over Western and Central Europe, significantly increased starting in the second half of the 16th century. During the 17th–18th centuries, the demography of Iaşi continued to be positive, although the city was often attacked by Tatars, Ottomans, Cossacks, and the Polish. In the urban life evolution of Moldova, the 17th century was marked by crisis and economic decline caused by the southeastern orientation of trade, oppressive fiscality, numerous years of drought, famines and epidemics [62].

Regarding treponematosis, the documents written in the 18th and 19th centuries provide information on the health status of the population. Accounts from foreigners and medical reports give details regarding the two neighboring countries of Moldavia and Wallachia. For example, the foreign traveler Andreas Wolff, who visited Moldavia in

1780, mentioned that "*. . .for many years now these people suffer so much because of the disease of syphilis. . .*" [63]. According to Radu et al. [55], the historian Franz Sulzer mentioned the high prevalence of syphilis in both countries, Moldavia and Wallachia, in his book *Geschichte des transalpinisches Daciens (1782)*.

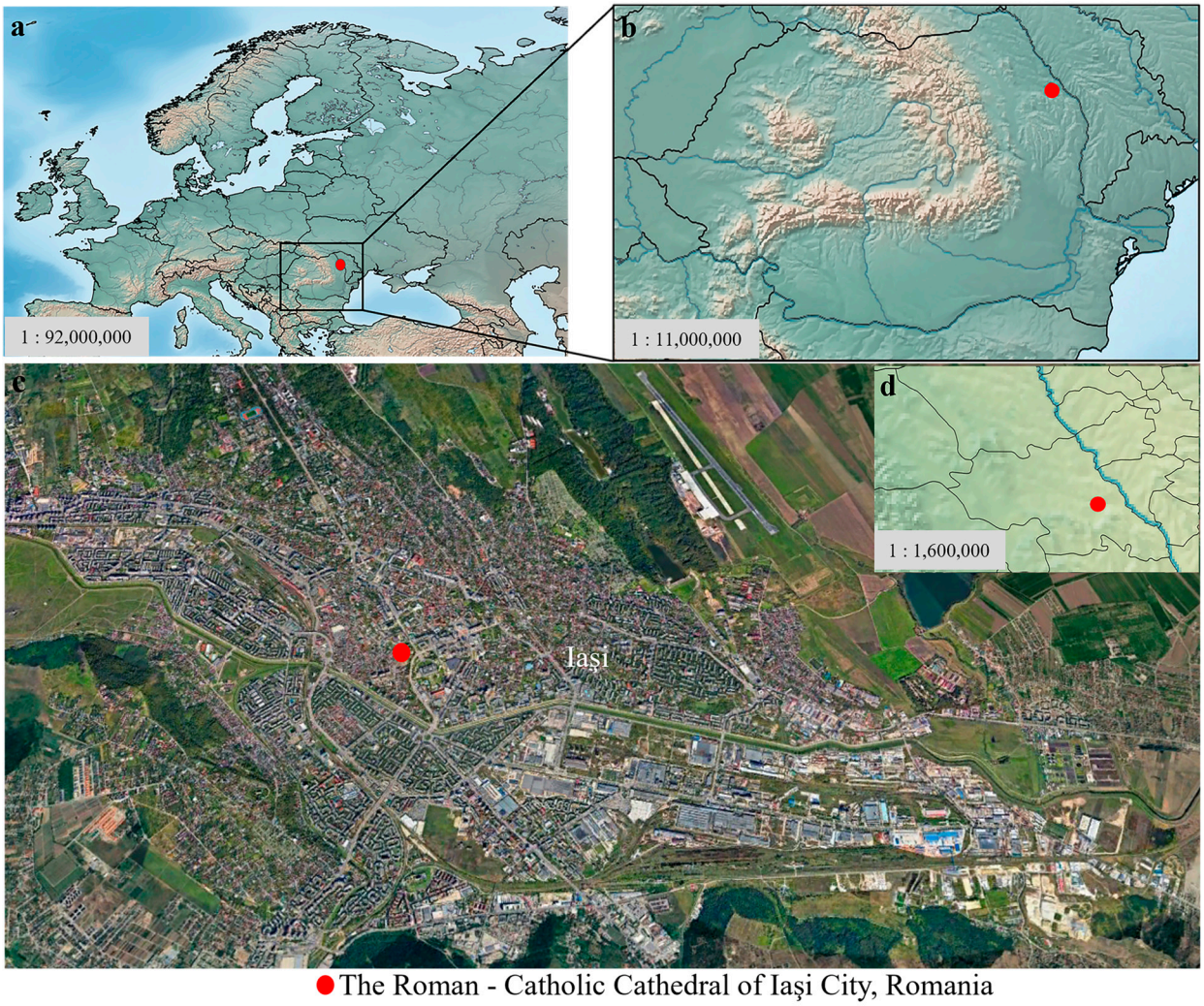


Figure 1. Localization of the Roman Catholic Cathedral in Iași, Romania: (**a**) geographic position within Europe; (**b**) positioning of the cathedral at the national level; (**c**) placement of the cathedral within the urban and territorial structure of Iasi city; (**d**) spatial location of the cathedral within the city of Iasi (Map source: https://www.simplemappr.net/, accessed on 13 February 2026).

3. Material and Methods

3.1. Material

In 1995, a necropolis dated to the 15th–19th centuries was discovered at the "Adormirea Maicii Domnului" City. The material exhumed from this necropolis is represented by 89 inhumation skeletons coming from individual tombs and reburials [64]. The bodies' orientation was according to the Christian ritual (i.e., east–west). The dating of the skeletons was made only according to general historical sources [58,65] and archaeological contexts [59,60], and there were reasons why it was not possible to place these individuals within a smaller time frame. The age at death and the sex were estimated in a previously paleodemographic analysis achieved by Groza et al. [64]: 68 adults (76.40%) and 21 subadults (23.60%); as adult individuals, 32 are females (47.05%), and 36 are males (52.94%).

In this study, we focus on three adult skeletons, which show pathological modifications suggestive of an inflammatory condition. One skeleton, codified with M40, comes from an individual grave, and the other two, codified R26 and R30, come from reburials. In the absence of genetic tests and archaeological markers, it is not possible to determine whether the three skeletons belonged to related individuals or if they lived simultaneously.

Bone preservation was assessed using the Anatomical Preservation Index (API) [66]. API is calculated as the average preservation score from scores of all bones, where each score represents the percentage of bone preserved relative to the total number of bones in the skeleton. Each bone is classified into one of six categories, ranging from absent to fully preserved, based on the criteria defined by [66].

3.2. Macroscopic and Stereomicroscopic Examination

The study of bone lesions was done by macroscopic examination of the cortical surface and using a stereomicroscope Carl Zeiss Stemi 2000-C (Carl Zeiss Mikroskopie, Jena, Germany) with a Canon Power Shot SX70 HS (Canon Inc., Tokyo, Japan) attached. Subsequently, selected skeletal remains were examined using medical imaging by radiography (X-rays) and tomography (CT scans). The radiographs were taken with KaVo OP 3D Pro (Palodex Group OY, Tuusula, Finland), medical radiological equipment, at 66.3 kV and 5 mA. For the CT study, SOREDEX SCANORA 3Dx equipment (SOREDEX, Tuusula, Finland) was used; scanning parameters were as follows: 90 kV and 4 mA. For the volume rendering of the selected objects, the software OnDemand3D (Cybermed Company, Seoul, Republic of Korea, version 1.0.0.1) was employed. Slices were singled out to better analyze internal bone structure. As they can discern changes in the bone cortex, the CT scans and X-rays have been used to make a case of probable treponematosis in comparison with other systemic infectious diseases such as pyogenic osteomyelitis or tuberculosis [24].

The differential diagnosis followed the guidelines of Aufderheide and Rodríguez-Martín [21], Hackett [20], Ortner [24], Roberts and Manchester [33], Steinbock [23] and Waldron [67], which offer detailed descriptions and images on lesion patterning and disease progression.

3.3. Microscopic Examination

The bone tissue samples were collected from the left femur (middle diaphysis) and right humerus (distal diaphysis) of the M40 skeleton, and right humerus (distal diaphysis) and left fibula (proximal diaphysis) of the R30 skeleton, with analysis focusing on the analysis of newly formed bone tissue and on the underlying cortical bone. The study on human skeletal remains was done in accordance with the American Association of Biological Anthropology ethical guidelines (e.g., to work for the long-term conservation of the archaeological records, to preserve opportunities for future research, to ensure preservation of data for use by posterity). Regarding the histological approach of this study and to minimize destructive sampling, only one sample from the aforementioned bone was collected and subjected to analysis. Bone samples were collected in a 'V' shape with a thickness of a maximum of 5 mm using a Dremel 3000 multi-tool (Dremel, Mount Prospect, IL, USA) equipped with a diamond-cutting wheel [68,69]. The bone samples were embedded in EpoThin 2® epoxy resin and hardener (Buehler) (Illinois Tool Works, Lake Bluff, IL, USA) and prepared using an IsoMet 1000 precision sectioning saw (Buehler, Lake Bluff, IL, USA) [68,70,71]. Mounting was performed using a small amount of epoxy resin, followed by a new stage of grinding and polishing, and completed with the placement of a coverslip over the sample [70]. The bone sections were examined using a Leica TCS SPE DM 5500Q microscope (Leica Microsystems CMS GmbH, Mannheim, Germany) equipped with a Leica DFC 290 camera (Leica Microsystems, Heerbrugg, Switzerland) as well as

a Carl Zeiss Axio Imager A1m microscope (Carl Zeiss MicroImaging GmbH, Göttingen, Germany) equipped with a Canon Powershot G9 (Cannon Inc., Tokyo, Japan) attached.

Considering the impact of postmortem processes on histological analysis, an assessment of the bone tissue quality was conducted using the Oxford Histological Index (OHI) [72–74]. The index comprises six stages, from 0 to 5, based on the extent of unaltered bone and the preservation of bone histological features such as osteons, bone lamellae, and osteocyte lacunae. The microbial alterations were microscopically recorded based on a presence/absence scale; although the non-Wedl microscopic focal destruction (mfd) types of microbial alteration could have different microarchitectures, they are considered indicators of the same bacterial attack [75,76].

4. Results

4.1. Preservation State of Skeletons

The Anatomical Preservation Index (API) values are 60% for M40, 50% for R26, and 43% for R30, indicating a decreasing gradient of bone preservation across the three skeletons. Based on the classification system of Bello [66], M40 is placed in Class 4, indicative of moderate preservation; R26 falls within the lower range of Class 4 to the upper range of Class 3; and R30 is categorized in Class 3, reflecting a comparatively lower representation of skeletal elements.

In all cases, axial and proximal appendicular elements are better preserved than distal elements, particularly those of the hands and feet, which display greater degrees of loss. The state of skeletal preservation and the locations of identified pathological lesions are presented in Figure 2.

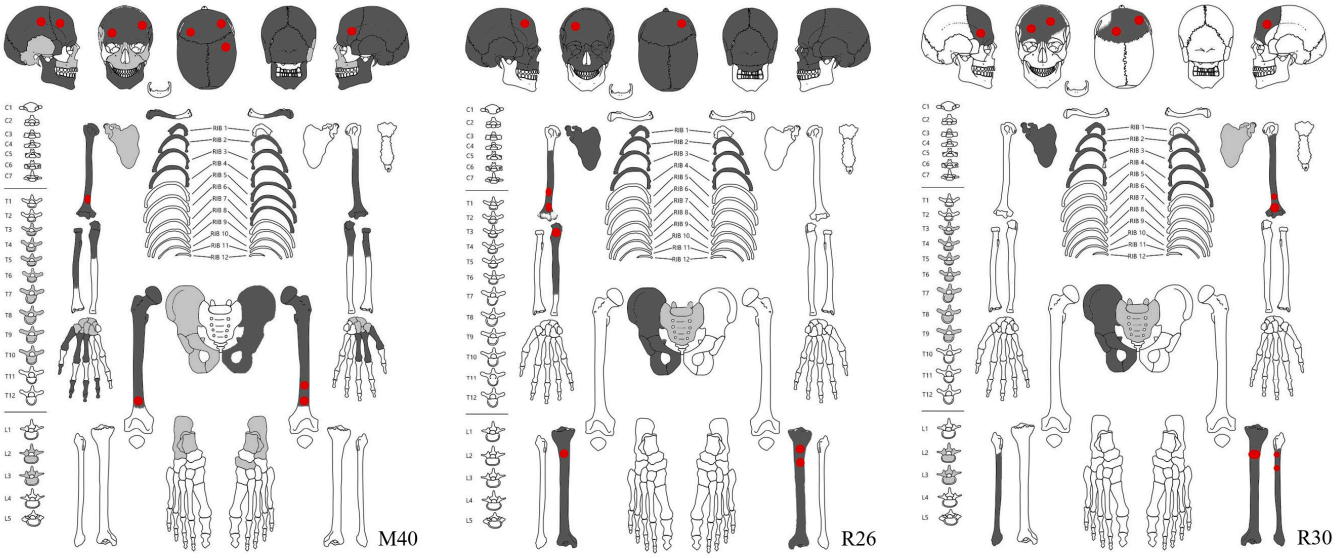


Figure 2. State of preservation for the skeletons M40, R26 and R30: dark grey—skeletal element is complete or nearly complete; light grey—skeletal element is present but fragmented; white—missing skeletal elements; red dots—locations of identified pathological lesions (Source image: INTERPOL DVI Form—Unidentified Human Remains).

4.2. Skeleton M40

4.2.1. Macroscopic Description of Pathologies in Skeleton M40

Skeleton M40 (female young adult of 30–35 years old) displays multiple pathological bone changes consisting of both proliferative and destructive lesions, with evidence of the body's attempts at repair and remodeling. The lesions are located in both cranial and postcranial bones (Figure 2). The cranial vault presents lesions on the frontal and the

right parietal; they have a serpiginous, "worm-eaten" appearance, with diffuse resorption and nodulation, as the confluence of several clustered pits resulted in large cavities. The ectocranial surface is mostly affected, and the diplöe is involved as well (Figure 3a,b). Each lesion has an osteolytic depression at the center and reactive, raised bony processes at its margins (Figure 3c). The computed tomography (Figure 3d,e) reveals that the lesions spread throughout the diplöe, producing an irregular surface.

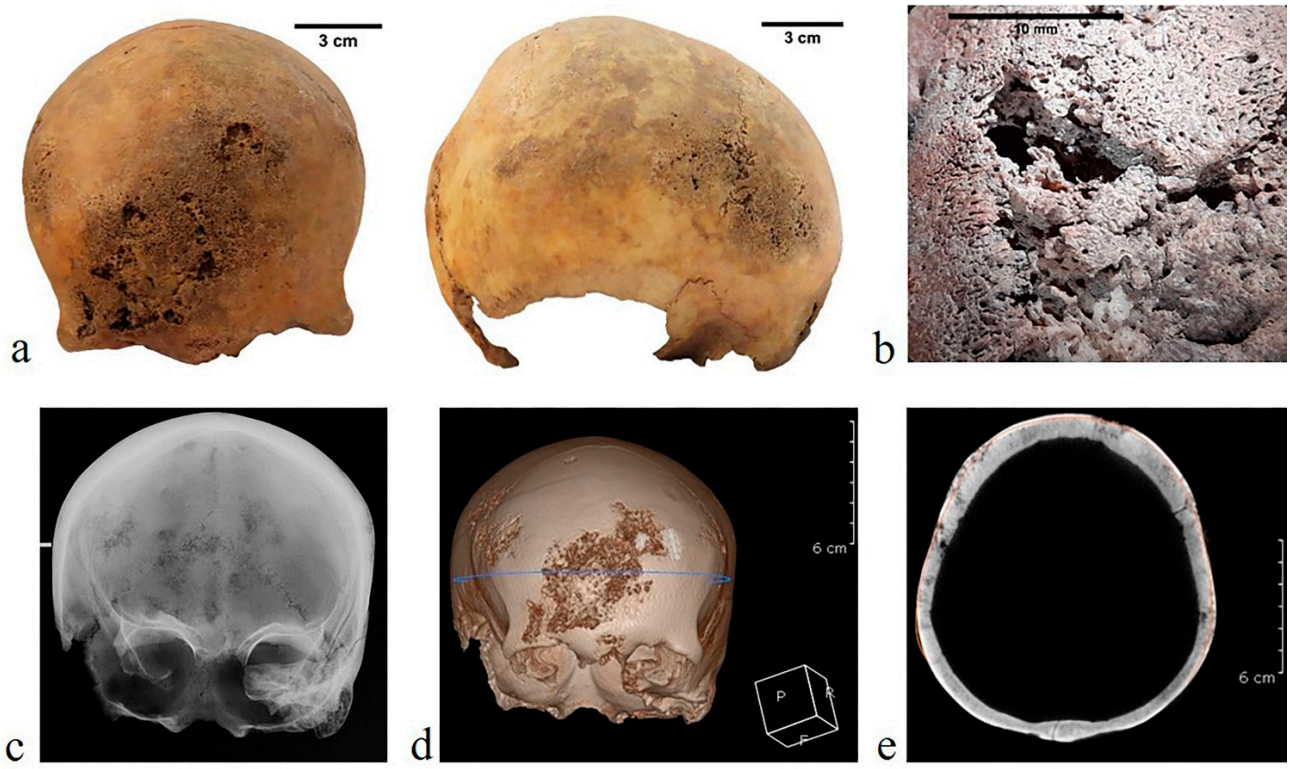


Figure 3. Cranial vault of M40: (**a**) macroscopic view of the lesions recorded in the frontal bone (anterior view) and right parietal bone (lateral view); (**b**) stereomicroscopic view of ectocranial lesions in the frontal bone (superficial focal cavitation perforating into the diplöe, depressed lesion); (**c**) X-ray of the frontal bone, lytic lesions; (**d**) CT scan 3D, cranial vault (lesions in the frontal bone—anterior view); (**e**) CT, cranial vault, lesions on axial section. Blue line in (**d**) indicates the level of the section shown in (**e**).

We also note, at the skull, the presence of two wormian bones on the lambdoid suture and dental pathologies. Dental caries (i.e., interproximal, cervical and root caries) affected the upper second molars (M^2), left lower first and second molars (M_1, M_2) and the right lower third molar (M_3). Supragingival dental calculus is reported on the right upper canine (C).

In the postcranial skeleton, pathological changes are identified on the right humerus and on the femora. New bone formation with a rugose porous surface and cavitations appears on the right humeral distal diaphysis (Figure 4a,b). X-ray and CT scans show a rugose, deteriorated structure. The transversal section reveals the alteration of the medullary cavity, which is significantly narrowed (Figure 4c–e).

Both femora have bone expansions with coarse striations and pitting on the distal half of the diaphysis (Figure 5a,b). The periosteal origin of these bony deposits is clearly seen in the longitudinal sections (Figure 5d,e). That, and the coarse surface pattern, would indicate a rapid deposition process. The limit between the changed and unchanged bone is clear (Figure 5c), and in the literature, it is mentioned that the affected tissue is often finely striated [20].

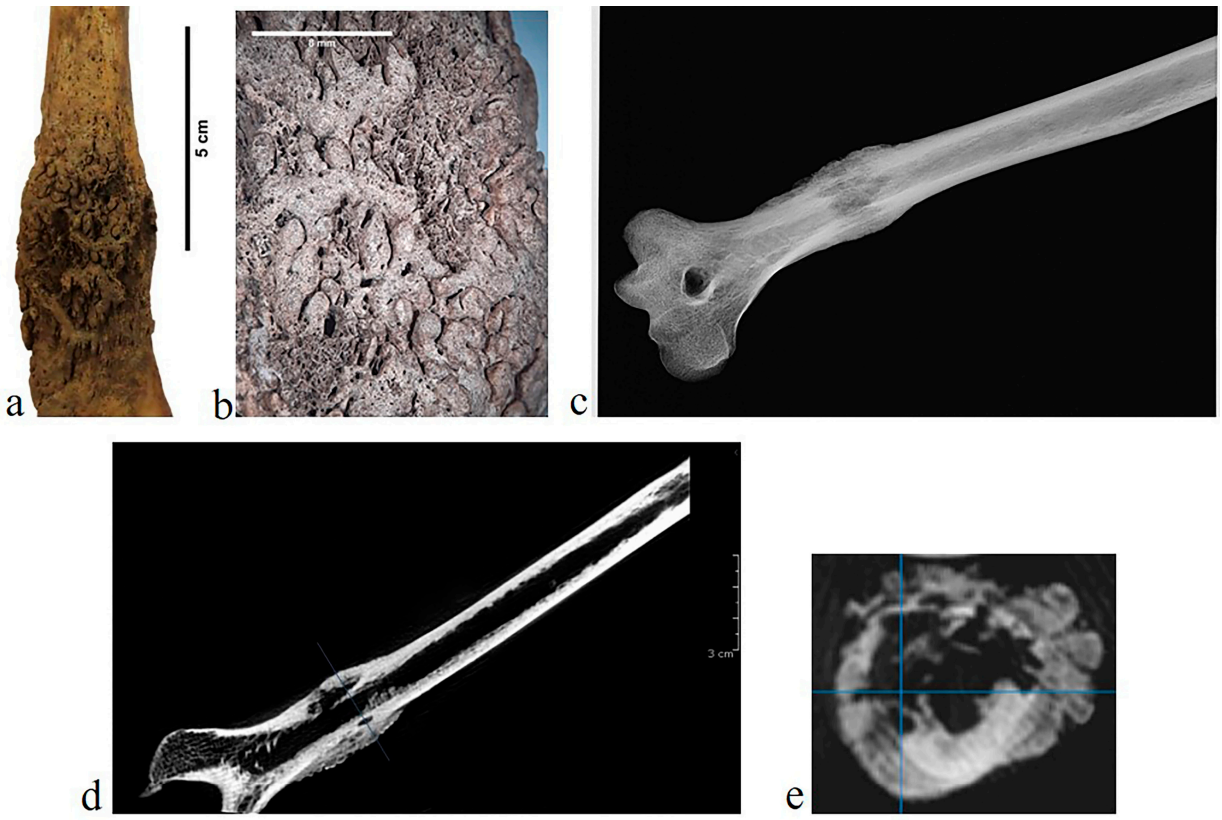


Figure 4. Right humerus of skeleton M40: (**a**) macroscopic view of the lesions recorded on the distal diaphysis (posterior view); (**b**) stereomicroscopic view (posterior view); (**c**) X-ray of the distal diaphysis; (**d**) CT, longitudinal section of the distal diaphysis; (**e**) CT, transversal section on the distal diaphysis. Transversal line in (**d**) indicates the level of the section shown in (**e**).

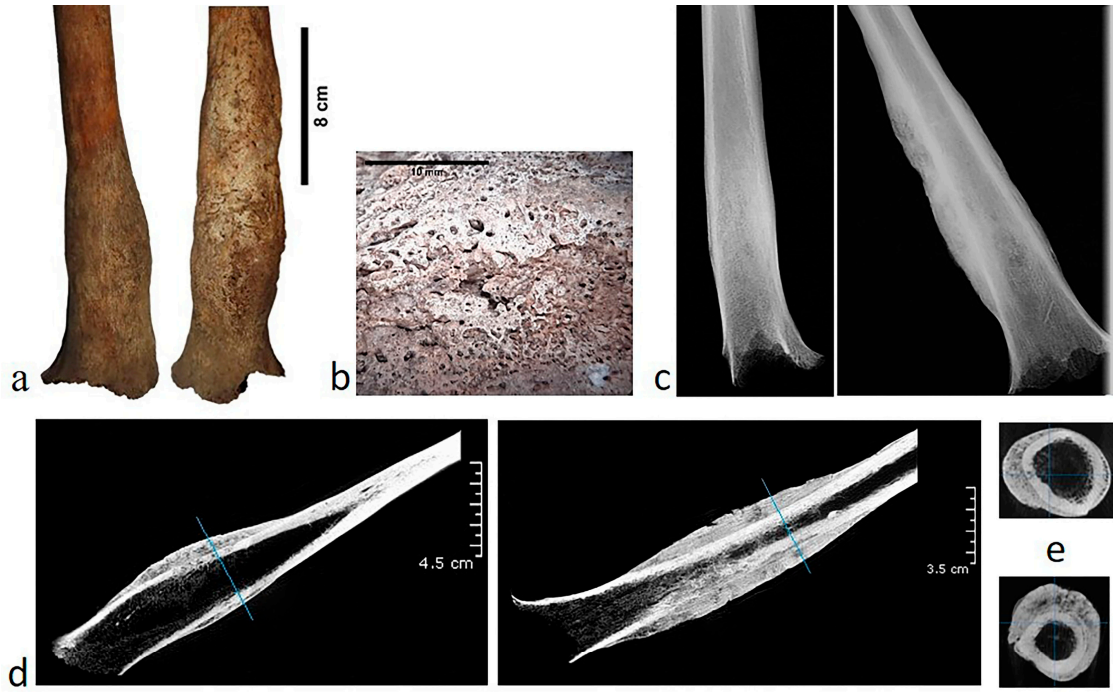


Figure 5. Femora of skeleton M40: (**a**) macroscopic view of the lesions recorded on the distal diaphysis (anterior view); (**b**) stereomicroscopic view of the distal diaphysis (anterior view); (**c**) X-ray of the distal diaphysis; (**d**) CT, longitudinal section of the distal diaphysis (anterior view) and location of transversal section ((**e**) superior view). Blue lines in (**d**) indicate the levels of the sections shown in (**e**).

4.2.2. Microscopic Description of Pathologies in Skeleton M40

The femur bone sample collected from the M40 human skeleton showed good preservation in archaeological context (OHI = 4). Only a few areas of destruction are visible, and locally, several zones with taphonomic infiltration and inclusions were identified. In addition, within the cortical bone, the osteocyte lacunae, osteons and interstitial lamellae are very well preserved.

The cross-section through the left femur suggests the presence, on the external surface of the bone, of periosteal new bone formed by apposition onto the external surface of the diaphysis (Figure 6a). Morphologically, the periosteal new bone formation (PNBF) resembles a "ploster-like" structure with "crypt" gaps but with two types of bone tissue (lamellar and woven bone) (Figure 6a–c).

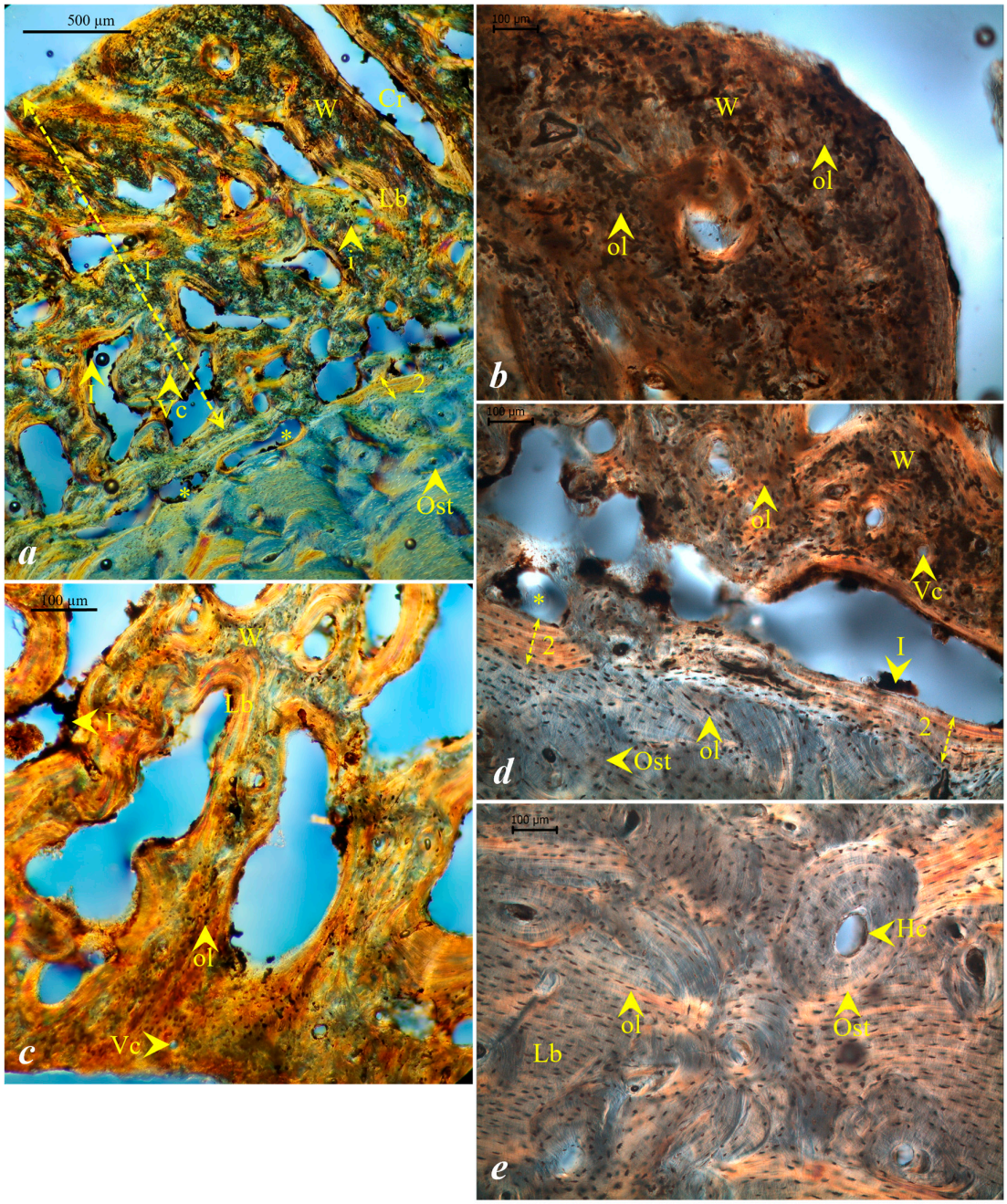


Figure 6. Cross-section through the femur belonging to the M40 skeleton (OHI = 4): (**a**) overview of the newly formed tissue ("polster-like") (1) and cortical bone (POL), 50×; (**b**) detail of woven bone

within the newly formed tissue (DIC), 100×; (**c**) detail of the proliferative osseous formation showing both bone lamellae and woven bone (POL), 100×; (**d**) "grenzstreifen" (2) separating the cortical bone from the new proliferative bone structure (DIC), 100×; (**e**) compact bone apparently unaffected by osteolysis (DIC), 100×: Cr—crypt; Hc—Haversian canal; I—taphonomic inclusions; Lb—lamellar bone; Ol—osteocyte lacunae; Ost—osteon; Vc—vascular canals; W—woven bone tissue; *—sinuous lacunae; 1—periosteal newly formed tissue; 2—"grenzstreifen", DIC—differential interference contrast, POL—polarized light, OHI—Oxford Histological Index.

Within the PNBF, remnants of vascular canals are noted, an indicator of the inflammatory process. Several sinuous lacunae were identified (Figure 6a,d). At the transition between PNBF and the cortical bone, a discontinuous lamellar structure was observed, separating the original surface of the femur shaft from the external newly built bone formation (Figure 6a,d), resembling the structure described by Schultz [77]—"grenzstreifen" or "grenzlinie". The underlying compact bone tissue appears unaffected by osteoclastic activity, with very well-preserved osteons and interstitial bone lamellae (Figure 6e).

The tissue sampled from the right humerus belonging to the M40 skeleton showed a very good taphonomic preservation (OHI = 4), with some observable taphonomic inclusions (Figure 7a). The newly formed tissue was characterized by numerous cavities (areolae), vascular canals, woven bone and lamellar bone, occasionally displaying a villous morphology with "crypt" gaps (Figure 7b,c). A lamellar structure—"grenzstreifen"—was observed in the humerus cross-section (Figure 7a). The compact bone tissue shows numerous resorption lacunae resulting from osteoclastic activity, with several Howship lacunae, producing a lace-like morphology that affected the cortical bone (Figure 7d,e).

4.3. Skeleton R26

4.3.1. Macroscopic Description of Pathologies in Skeleton R26

Skeleton R26 (male middle adult of 35–40 years old) shows, on the skull, clustered pits in the frontal bone (Figure 8a,b). The radiography of the skull indicates lytic lesions on the frontal (Figure 8a), and the CT shows small lytic areas on the outer table of the frontal region (Figure 8b,d) and in the zygomatic bones (Figure 8b,d). A long metopic suture extends from the coronal suture to the glabella. Dental pathologies are also present: dental caries (cervical caries) affecting the left upper third molar (M^3) and supragingival dental calculus on the left upper premolars (P^1, P^2) and the left upper first molar (M^1).

In the postcranial skeleton, lesions are observed on the right humerus, right ulna and tibiae. The humerus and ulna show massive periosteal reaction involving osseous thickening, nodulation, and hollow cavitations (foci of necrotic tissue surrounded by reactive bone) (Figure 9a,b). Both bones have lytic cavitations and probable gummatous lesions, with necrotic zones encircled by reactive bone growth (Figure 9c–e). The transversal section revealed the involvement of the medullary cavity, which is narrowed (Figure 9f).

The tibiae are both affected by the pathologic process (more lesions on the left tibia). The external surface of the tibiae is altered showing nodes and rugosity (Figure 10a). The lower border of the nodes is defined and slightly striated (Figure 10c). In the literature, it is mentioned that the most prominent changes are often on the proximal medial surface of the tibia [20], a situation reported in the case analyzed by us. In the radiography and the CT longitudinal section, a boundary line is seen between the original cortex and the bony deposit (Figure 10b,d). The narrowed medullary cavity can be seen in the transversal section (Figure 10e).

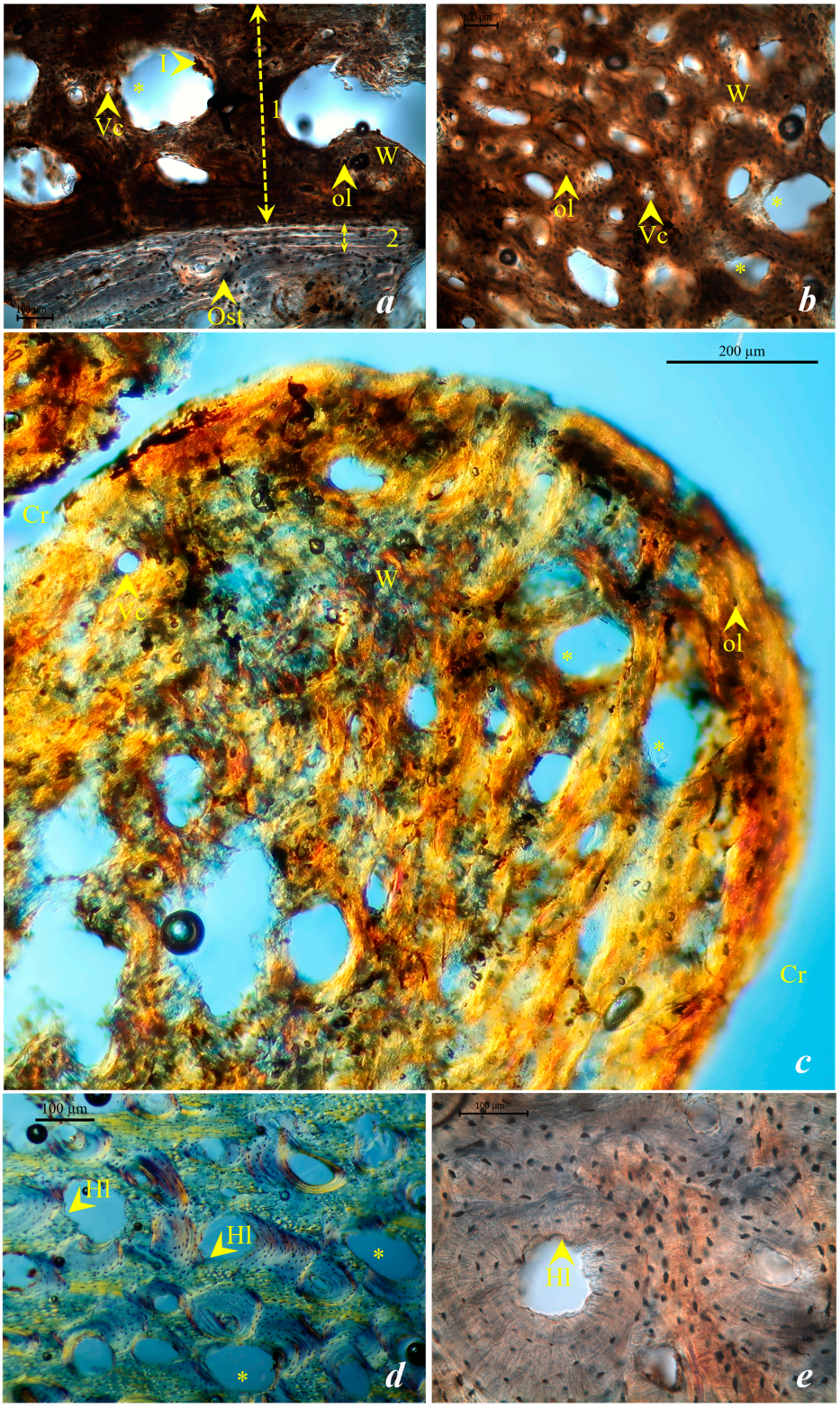


Figure 7. Cross-section through the humerus belonging to the M40 skeleton (OHI = 4): (**a**) overview of the newly formed tissue (1) and "grenzstreifen" (2) (DIC), 100×; (**b**) detail of woven bone within the newly formed tissue (DIC), 100×; (**c**) detail of the PNBF villous morphology (POL), 50×; (**d**) cortical bone affected by osteolysis (DIC); (**e**) detail of compact bone showing Howship lacunae, 200×: Cr—crypt; Hl—Howship lacunae; I—taphonomic inclusions; Ol—osteocyte lacunae; Ost—osteon; Vc—vascular canals; W—woven bone tissue; *—sinuous lacunae; 1—periosteal newly formed tissue; 2—"grenzstreifen", DIC—differential interference contrast, POL—polarized light, OHI—Oxford Histological Index.

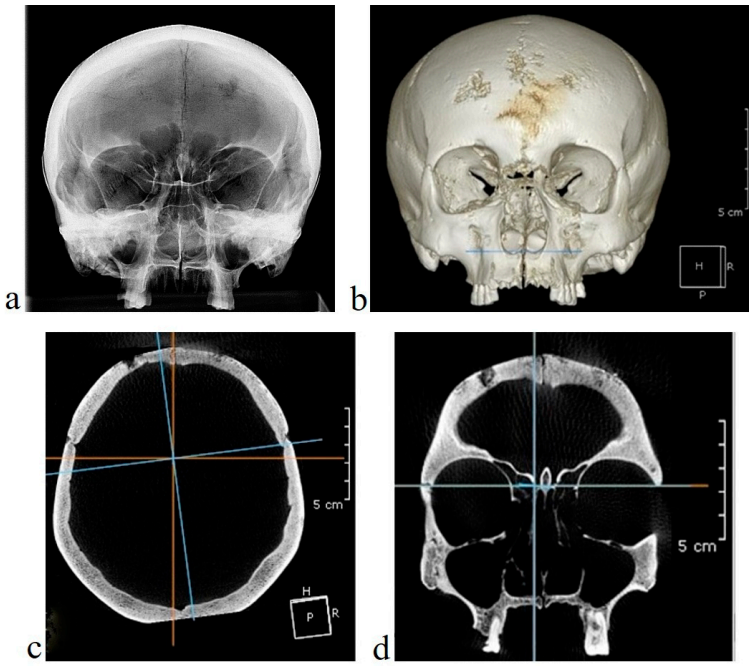


Figure 8. Cranium of skeleton R26: (**a**) X-ray of the cranium, lytic lesions; (**b**) CT scan 3D, lesions in the frontal and zygomatic bones—anterior view; (**c**) CT, axial section showing lesions in frontal and parietal bones; (**d**) CT, coronal section with lesions in frontal and zygomatics.

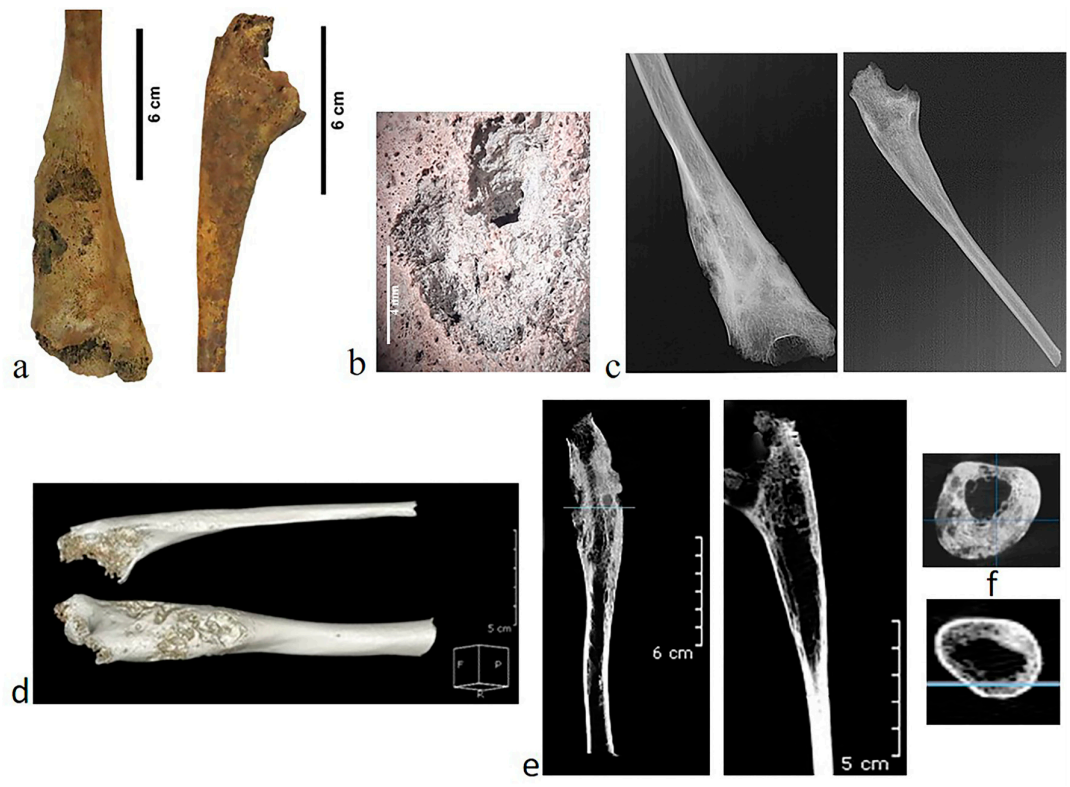


Figure 9. Right humerus and right ulna of skeleton R26: (**a**) macroscopic view of the lesions in the right humeral distal diaphysis (anterior view) and right ulna proximal diaphysis (lateral view); (**b**) stereomicroscopic view of the right humeral distal diaphysis; (**c**) X-ray of the right humeral distal diaphysis (anterior view) and right ulna proximal diaphysis (lateral view); (**d**) CT scans 3D, right humeral distal diaphysis (anterior view) and right ulna proximal metaphysis (lateral view); (**e**) CT, longitudinal section of right humerus, and right ulna; (**f**) CT, transversal sections of humerus diaphysis and ulna diaphysis. Transversal line in (**e**) indicates the level of the section shown in (**f**).



Figure 10. Tibiae of skeleton R26: (**a**) macroscopic view of the lesions in the proximal diaphysis (posterior view); (**b**) X-ray of the proximal diaphysis (posterior view); (**c**) CT scans 3D, lesion in the proximal diaphysis; (**d**) CT, longitudinal section of the proximal diaphysis; (**e**) CT, transversal section. Transversal lines in (**d**) indicate the levels of the sections shown in (**e**).

4.3.2. Microscopic Description of Pathologies in Skeleton R26

The histological analysis of pathological bone (i.e., humerus) belonging to the R26 skeleton was the focus of a recently published study [78]. According to the study, the PNBF is limited in extent, being composed predominantly of primary bone tissue, with only a few areas being composed mainly of bone lamellae. In addition, a very fine lamellar demarcation between the PNBF and cortical bone was identified only in a few areas [78]. The cortical bone is characterized by the presence of a small number of osteons with a trabecular-like appearance. The observed tissue morphology is more likely associated with increased local porosity than with osteoblastic apposition secondary to periosteal inflammation (periostitis); instead, it most plausibly reflects inflammation of the bone tissue itself (osteitis) [78].

4.4. Skeleton R30

4.4.1. Macroscopic Description of Pathologies in Skeleton R30

Skeleton R30 (female middle adult of 35–40 years old) has pathological changes in the frontal bone as several focal cavitations penetrating into the diploë and affecting the inner table. There are also compact bone depressions with radial grooves that create a stellate pattern consistent with *caries sicca* (Figure 11a,b). The presence of *caries sicca* in the cranial vault is considered by some authors [20,21] as a pathognomonic sign of acquired syphilis or, to others, a sign of endemic treponematosis (e.g., bejel, yams) [24]. The numerous lytic lesions contrast with areas resulting from destruction followed by repair of bone tissue. Most margins of the lesions are smooth with evidence of healing, with radial scars

particularly visible in the frontal bone. The radiological and computed tomographical examinations show that the lesions spread throughout the diplöe, producing an irregular aspect (Figure 11c–f).

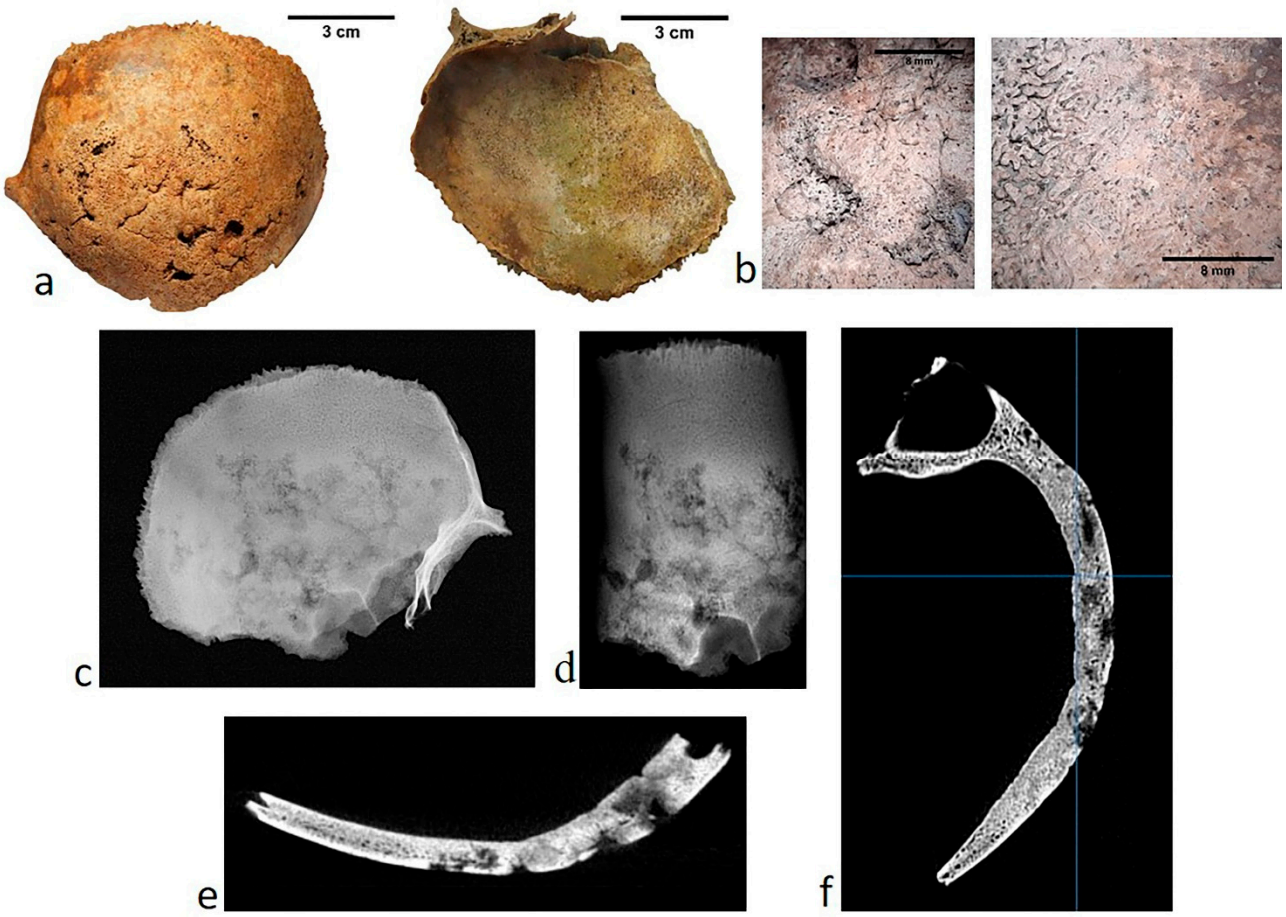


Figure 11. Frontal bone of skeleton R30: (**a**) ectocranial and endocranial macroscopic view of the lesions; (**b**) stereomicroscopic view of ectocranial and endocranial lesions (superficial focal cavitation perforating into the diplöe and stellate grooves around a healed, depressed lesion); (**c**) X-ray, lytic lesions; (**d**) CT, panoramic view of the frontal bone; (**e**) CT, axial section of the frontal bone; (**f**) CT cross-section of the frontal bone.

The postcranial lesions in this skeleton are concentrated on the left side of it. The bones affected in this case are the left humerus, left tibia and left fibula. In the distal diaphysis and metaphysis of the left humerus, periosteal appositions and small areas of focal destruction are present (Figure 12a,b). CT scan investigation of the affected humerus reveals lytic areas, a thick periosteal reaction and narrowing of the medullary cavity (Figure 12c–e).

The left tibia and fibula are both affected by a pathologic process (Figure 13). On the left tibia (Figure 13a–e), a granulomatous lesion appears as a striated nodule with a central gummatous cavitation [20]. X-ray and CT scan of the left tibia show a zone of density, thickened cortical and narrowed medullar cavity (Figure 13c–e). In the left fibula, rugose expansions are present. The surface pattern is a mixture of rippling and trabeculation with some striation and pitting; in places, the surface is rough and granular (Figure 13a,b). The radiology and computed tomography highlight deteriorated appearance rugose and thickened cortical layers (Figure 13c–e). The transversal section reveals the aspect of the medullary cavity, which is significantly narrowed and partially obliterated (Figure 13e).

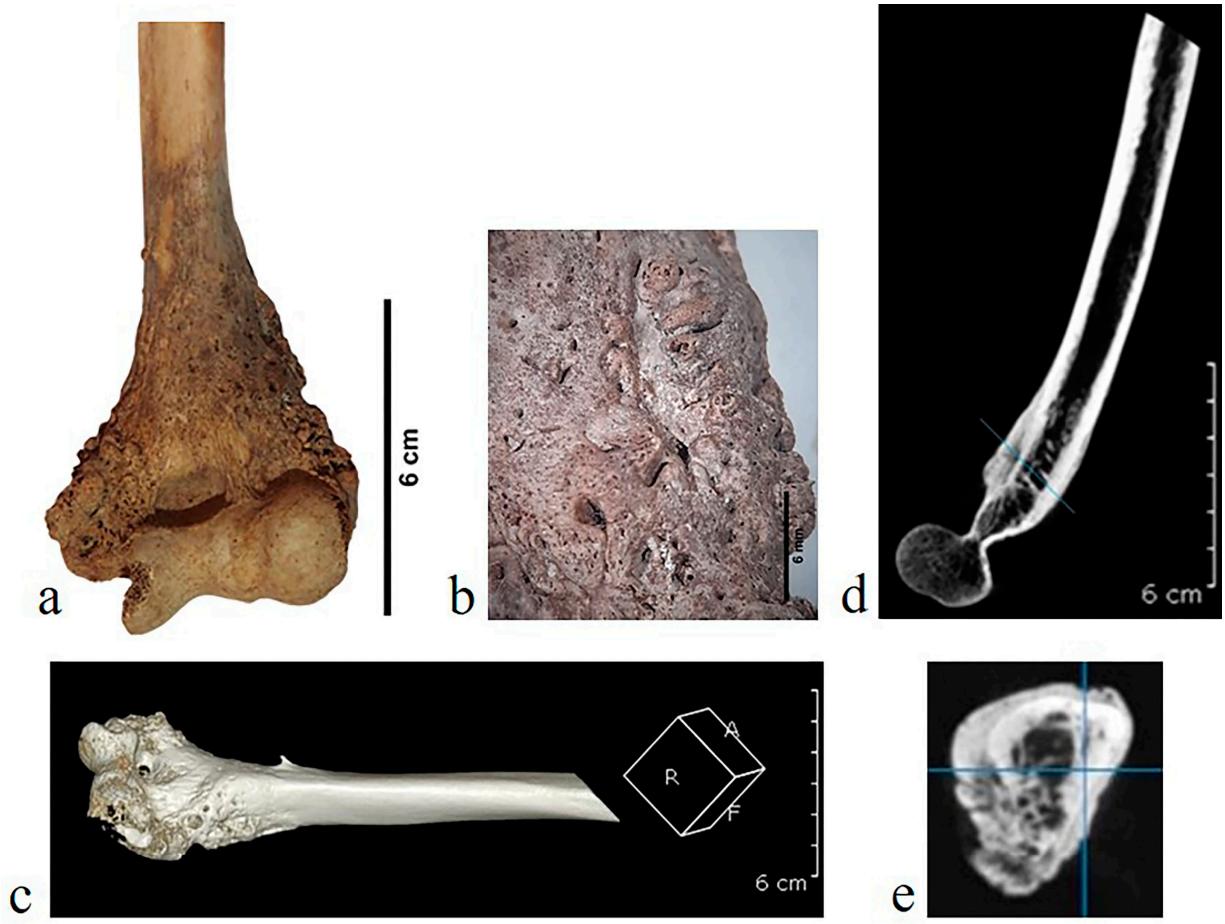


Figure 12. Left humerus of skeleton R30: (**a**) macroscopic view of the lesions recorded in the distal diaphysis and metaphysis (anterior view); (**b**) stereomicroscopic view of the distal metaphysis (anterior view); (**c**) CT scan 3D of the distal diaphysis and metaphysis (anterior view); (**d**) CT, sagittal section of the distal diaphysis and metaphysis (lateral view); (**e**) CT, transversal section (superior view). Transversal line in (**d**) indicates the level of the section shown in (**e**).

4.4.2. Microscopic Description of Pathologies in Skeleton R30

Bone tissue sampled from the left fibula showed good preservation with evident osteons, bone lamellae and osteocyte lacunae (OHI = 4). In some areas of the PNBF and cortical bone, some isolated taphonomic inclusions and infiltrations were identified. The PNBF formed on the external surface of the left fibula shows a slightly different morphology compared to the PNBF of the M40 samples. The cross-section taken from the fibular hyperostosis suggests a newly formed tissue with a villous and polypoid morphology, with both immature and lamellar bone tissue being present (Figure 14a–c). The development of newly formed bone tissue as a result of periosteal inflammation oriented perpendicular to the cortical region, together with their morphology, may represent an indicator of osteoblastic activity with rapid formation during an acute stage of treponematosis. The shape and orientation of the tissue within the polypoid structure may indicate recurrent periostitis (Figure 14b). Further support for an acute stage of the disease may be provided by osteoclastic activity in the cortical bone. In this area, numerous bone resorption lacunae are observed in proximity to the separation zone between the newly formed tissue and the cortex as well as numerous Howship lacunae (Figure 14e,f). Osteolysis is evident across the entire cortical surface (Figure 14g), extending to the endosteal surface (Figure 14h). Several osteons affected by intense osteoclastic activity were also identified.



Figure 13. Left tibia and left fibula of skeleton R30: (**a**) macroscopic view of the lesions recorded in the proximal end of the bones (posterior views); (**b**) stereomicroscopic views of the proximal diaphysis (posterior views); (**c**) X-rays of the proximal tibia and fibula (posterior views); (**d**) CT, longitudinal sections of the proximal tibia and fibula (posterior views) (the line marks the transversal section); (**e**) CT, transversal sections of tibia and fibula (superior view). Transversal lines in (**d**) indicate the levels of the sections shown in (**e**).

In the right humerus histological sample, the newly formed tissue shows a more homogeneous development compared to that of the fibula, where villous and polypoid formations were identified. The humerus histological sample resamples a "polster-like" morphology; no bone parallel lamellae to the bone surface were identified. In this region, woven bone tissue was observed, together with numerous areas dominated by bone lamellae and osteons, suggesting a shift towards a chronic manifestation, with bone remodeling being present. Taphonomic inclusions were observed mainly within the PNBF tissue (Figure 15a). In addition, remnants of vascular canals were identified (Figure 15b). The cortical zone is separated from the newly formed tissue by a well-defined lamellar band (i.e., "grenzstreifen") (Figure 15d). Within the cortical region, numerous areas of bone resorption along Howship lacunae were identified. Also, interstitial bone lamellae, osteons, and osteons affected by osteolysis were observed (Figure 15c,e).

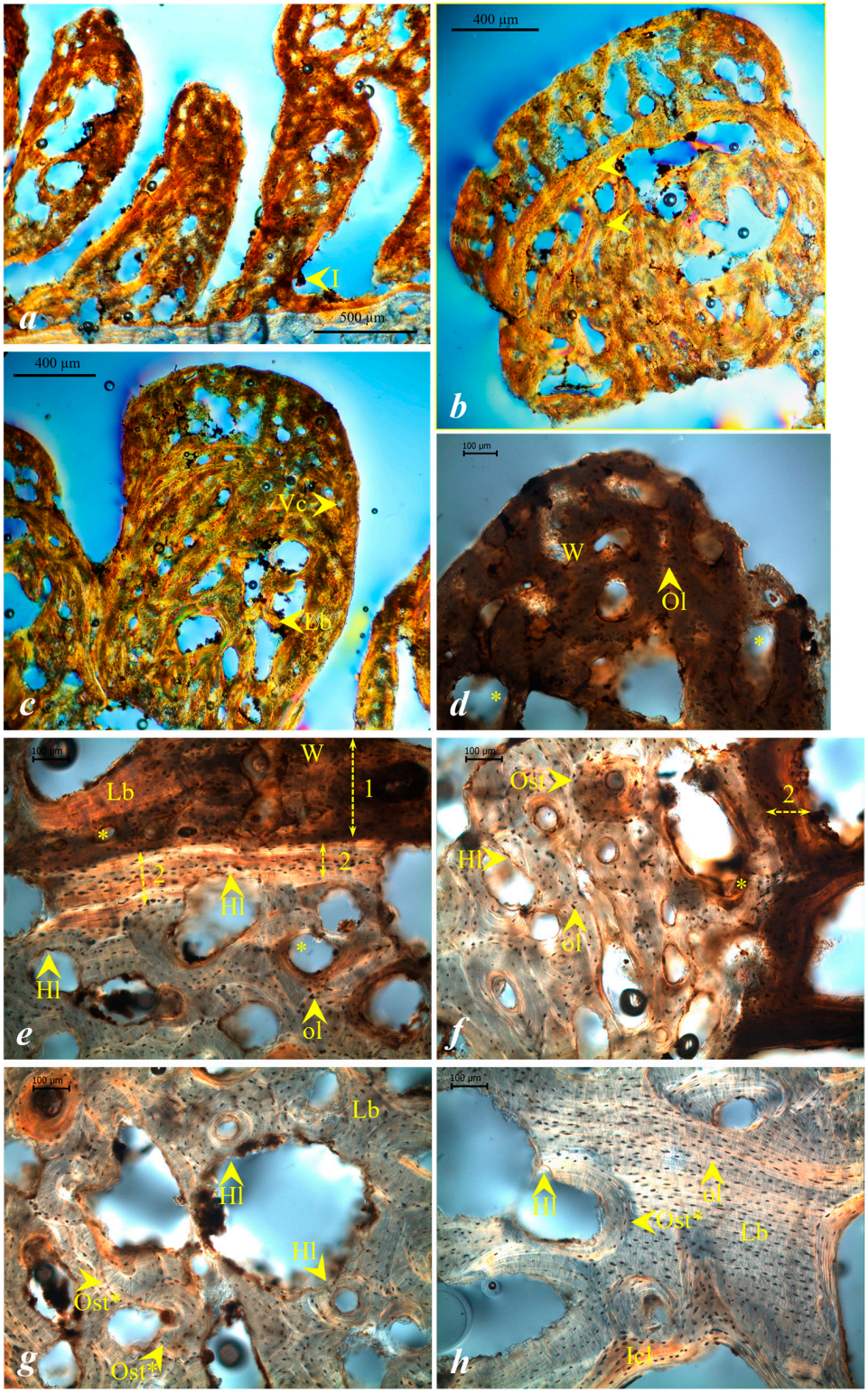


Figure 14. Cross-section through the fibula belonging to the R30 skeleton (OHI = 4): (**a**,**c**) villous-type of PNBF (POL, DIC), 50×; (**b**) polypoid-type of PNBF (POL), 50×: yellow arrowhead—orientation of the tissue may indicate recurrent perostitis; (**d**) detail of PNBF (POL), 100×; (**e**) PNBF (1) and "grenzstreifen" (2) (DIC), 100×; (**f**) cortical bone tissue (DIC), 100×; (**g**,**h**) details of cortical bone tissue with numerous resorption lacunae and Howship lacunae (DIC), 100×: Hl—Howship lacunae; icl—internal circumferential lamellae; I—taphonomic inclusions; Lb—Lamellar bone; Ol—osteocyte lacunae; Ost—osteon; Ost*—osteon affected by osteolysis; Vc—vascular canals; W—woven bone tissue; *—sinuous lacunae; 1—periosteal newly formed tissue; 2—"grenzstreifen", DIC—differential interference contrast, POL—polarized light, OHI—Oxford Histological Index.

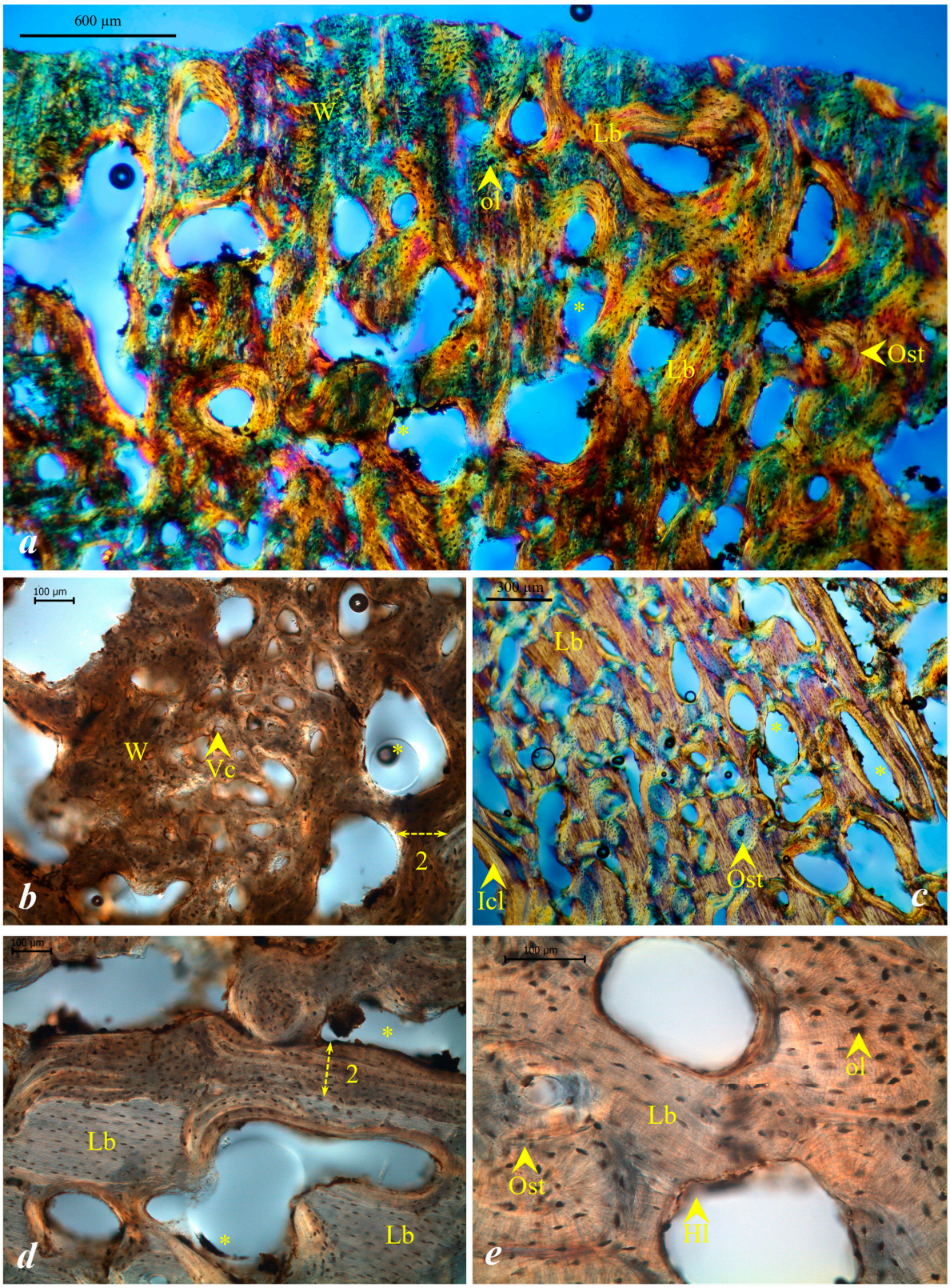


Figure 15. Cross-section through the humerus belonging to the R30 skeleton (OHI = 4): (**a**) PNBF overview (POL), 50×; (**b**) PNBF detail (DIC), 100×; (**c**) cortical bone tissue, overview (POL), 50×; (**d**) "grenzstreifen" (2) (DIC), 100×; (**e**) detail of cortical bone tissue with Howship lacunae (DIC), 100×: Hl—Howship lacunae; icl—internal circumferential lamellae; Lb—Lamellar bone; Ol—osteocyte lacunae; Ost—osteon; Vc—Vascular canals; W—woven bone tissue; *—sinuous lacunae; 2—"grenzstreifen", DIC—differential interference contrast, POL—polarized light, OHI—Oxford Histological Index.

5. Discussion

The three analyzed skeletons (i.e., M40, R26 and R30), discovered in the necropolis of the 15th–19th centuries from the "Adormirea Maicii Domnului" Roman Catholic Cathedral in Iași (Romania), display similar pathological lesions, suggesting that the group was probably suffering from the same disease.

The lesions identified in the skeletons, comprising abnormal bone formation and destruction, may be interpreted as a response to a chronic systemic disease [24,67]. To realize a differential diagnosis, the described lesions were compared with other pathological aspects that characterize other diseases, especially of infectious nature (i.e., Paget's disease of the bones, pyogenic osteomyelitis, tuberculosis, leprosy and treponematosis).

Paget's disease of bone is characterized by cortical thickening and sclerosis, and it is most likely caused by environmental and genetic factors [67]. Paget's disease occurs more commonly in the older age groups (>40 years), in males, and in populations of European descent, but it is rare in Africans and Asians [24]. The disease is not rare in a limited form, but its severe multi-osseous involvement is uncommon. This pathology is mainly located in the axial skeleton; in general, of the long bones, the femora and tibiae are the most affected [24,38]. On the cranium, the early Paget's disease lesions feature single or multiple resorptive areas with wavy margins and a porous surface [79]. As the disease worsens, extreme cortical and trabecular thickening/expansion as well as a mixture of lytic and sclerotic areas on the vault and other nonadjacent bones become apparent [24,79]. Lysis also takes place in the long bones and invariably begins in the subchondral bone and proceeds upwards or downwards. Affected bones show a V-shaped radiolucent area, which is usually called the "flame" sign. In the sclerotic (inactive) stage, the affected bones may become enlarged, and they feel heavier than their normal counterparts [55,67]. The skeletons at the "Adormirea Maicii Domnului" Roman Catholic Cathedral show degenerative lesions, but no Paget's disease features were observed, which led us to exclude this disease. In this study, CT scans do not display abnormal thickening of the bone cortex, especially on the frontal. Paget's disease is believed to be the abnormal activation of osteoclasts, leading to improper bone resorption and compensatory osteogenic sclerosis. This results in increased bone remodeling and mass [80,81], which is not the case with the lesions found in the analyzed skeletons.

Pyogenic osteomyelitis is an inflammatory response to an infection of bone marrow, caused usually by a pyogenic bacterium (*Staphylococcus aureus*) [21,24,51]. In the preantibiotic times, such infections would have been followed by bacteremia and the consequent hematogenous spread of the pathogens to more distant organs, including bones [33]. Lesions produced by this process rarely involve the cranium, but if they are present, they can spread through diplöic bone to other sites, including across sutures, although the occipital bone is often not affected [24]. These lesions mostly affect the diplöe and, to a lesser extent, the ectocranial surface [24,51]. The typical pathological evidence of chronic pyogenic osteomyelitis implies enlargement of the long bone shafts accompanied by sequestrated bones, involucrum and cloaca formation [20,24]. None of the three analyzed skeletons display sequestrum or involucrum, and the elements with abnormal, expanded cortical bone lack the hypervascularized surface or cloacal opening.

Tuberculosis is a chronic infectious disease caused by a bacterium of the *Mycobacterium* genus; *Mycobacterium tuberculosis* causes direct transmission between humans, usually through the respiratory tract. The infection develops in the lungs, and it can then spread through the bloodstream to distant organs, including bones [24,82]. Tuberculosis can affect any part of the skeleton, but unlike treponematosis, it is predisposed to the axial skeleton and particularly the vertebral bodies (especially the first lumbar vertebrae, but also the thoracic and cervical vertebrae) [24,82–84]. The infection affects the cancellous bone of

vertebrae and consists of osteolytic lesions that can lead to cavitation, ankylosis, vertebral collapse and angular kyphosis [85]. Tuberculosis can rarely affect the skull in adults, and in this case, the round and oval osteolytic lesions are no more than 2 cm in diameter, with reactive bone formation in the surrounding area [84]. Skeletal lesions in tuberculosis tend to be more destructive than formative. Reactive bone formation can be extensive in some cases, and the margins of destructive lesions in tuberculosis typically exhibit a sclerosis [24]. The morphological appearance of tuberculosis includes clustered pitting, circular osteolytic lesions and cavitation in bone areas with cancellous bone. New bone formation can occur in the rib, humerus, femur, tibia, fibula, and especially the epiphyses and metaphyses, with periosteal new bone formation being uncommon along the shafts of long bones [86,87]. In the skeletons analyzed in this work, the bone formation and degenerative lesions predominate, which allowed tuberculosis to be excluded as a diagnosis.

The distribution and the specificity of the lesions on the analyzed skeletons (M40, R26 and R30) highlight a probable treponematosis origin for the inflammatory process observed on the cranium and long bones of all three individuals. The pathological aspects reported in these cases are consistent with the characteristic traits of treponematosis, which usually affects multiple bones, are bilateral, and especially manifest in the ectocranial vault, the nasal region and the tibia [20,21,88]. The cavitating lesions in the analyzed skulls of the three subjects are similar to the pattern of *caries sicca* at different stages [20]. These lesions form a characteristic continuous area, covering the cranial vault surface with some degree of diplöe involvement, showing confluent cavitations with irregular, raised rims and concave walls; they are considered indicative of treponematosis [20,24,67,89]. The lesions reported in the postcranial skeletons (M40, R26 and R30) have a chronic aspect, and they correspond to a tertiary phase of treponematosis that usually occurs 2 to 30 years after the initial onset of symptoms [24,67].

Considering the estimated age at death (30–40 years), the initial infection likely occurred in early adulthood. The presence of advanced-stage lesions indicates a prolonged disease course, suggesting that these individuals, in great suffering, may have received care and support from the Catholic church, allowing them to survive with the condition for many years.

Considering the diagnostic features of treponematosis proposed by Hackett [20] and Harper et al. [14], the identified pathological aspects in the long bones could correspond to different phases of disease, as follows: phases five–six for the skeletons M40 and R26, with coarse striated and pitted bone surface; phase eight to nine for the skeleton R30, with rugose bone surface, moderate to severe. It is difficult to realize a differentiation between types of treponematosis based on bones, although some characteristics help to distinguish them.

Infection caused by the *Treponema* bacterium manifests in four very similar forms: pinta, yaws, endemic syphilis (treponarid/bejel) and acquired syphilis. Pinta, caused by *Treponema carateum*, is primarily a skin condition with no known skeletal involvement [88]. The other three treponematosis are caused by a subspecies of *Treponema pallidum,* and each of them can cause skeletal lesions [37,89], although there are some discernible differences in the epidemiology and clinical expression of the disease [88,90].

Yaws, caused by *T. pallidum pertenue*, most commonly has a childhood age of onset, with tertiary development starting at 5–10 years after the initial infection stage. The tertiary lesions of yaws are identical to those of acquired syphilis, the difference being in intensity [21], and also excepting that yaws can produce erosive joint involvement that may be unique among the treponematoses [34]. This form of the disease is believed to be transmitted primarily through direct contact via skin lesions, although the possibility of an insect vector has been raised [21,89]; it is restricted to humid climates [21,88,89].

Caused by *T. pallidum endemicum*, bejel appears early in life and affects people living in rural settings with poor hygiene. The infection is considered likely transmissible, and although the lesions in early stages are rarely seen, the disease does eventually affect the skin and bone tissues in its latter stages [23,79].

Acquired syphilis is a systemic illness that produces morpho-physiological changes in the body as chancres, rashes, and ulcers, followed in time by neurological damage, cardiovascular problems, and destructive lesions in the skin, mucous membranes, bones and internal organs [55,91,92]. It is transmitted most often via sexual intercourse, although congenital transmission from an infected mother to the fetus is also possible [21,23]. Clinically, syphilis can be described as having three stages (i.e., primary, secondary and tertiary) and a non-clinical latent phase [21,67]. Tertiary bone lesions of acquired syphilis are those most likely to be recognized in osteo-archaeological specimens. They may be regarded as falling into the following groups: gummatous; destructive and localized, non-gummatous; sclerotic and localized, often multiple; diffuse and combinations of these [20]. Lesions to the skull called *caries sicca* represent the most important diagnostic criteria of syphilis [20].

Considering the morphological characteristics and distribution of the lesions identified in the analyzed skeletons, it is most likely that the three subjects were affected by a treponematosis. The identified morphopathological pattern in all three individuals is similar to that described for acquired syphilis [21,22], mostly affecting the cranial vault (with *caries sicca* in different stages) and the postcranial skeleton (i.e., tibiae, fibula, femora, humerus and ulna). However, since there is no historical evidence indicating the presence of this disease, for a more accurate diagnosis, biomolecular analyses should be performed to support this hypothesis.

Regarding the histology of treponematosis, studies conducted by Schultz [77,93] led to the proposal of characteristic features including "polsters", "grenzstreifen" and sinuous lacunae, though these features have come under further scrutiny, questioning their specificity as indicators for treponematosis [68,94]. The histological features characteristic for treponematosis proposed by Schultz [93] could not be identified in the sections from the tibia of an individual affected by such disease, although macroscopically lesions indicated treponematosis [93]. Moreover, similar features were described in individuals with osteomyelitis, leprosy, and leg ulcers [77,93,95]. Several factors may account for the difficulty in identifying the histological features proposed for treponematosis, including severe postmortem tissue alteration that interferes with the identification of the features, methodological limitations related to the possibility that these features were not present in the specific area of the lesion sampled for sectioning, and the likelihood that such structures are not exclusively associated with treponematosis.

"Polsters" consist of "parallel lamellae arranged at the periosteal level in the form of pillow-like newly built bone formations", which are characterized by "blood vessels developed during the course of the inflammatory process" [77,95]. This formation is described as a homogeneous structure indicating a slowly developing, chronic process [77]. Newly formed bone tissue is also associated with periostitis in hematogenous osteomyelitis and can be described as having an irregular morphology reflecting rapid deposition and a high remodeling rate. Rudimentary, flat "polsters" can also occur in the skeletal manifestations of leprosy. "Grenzstreifen" (border line) is defined as a "band-like structure indicating the place of the original external surface of the shaft of a long bone" separating the newly formed bone tissue formed during inflammation from the cortical bone tissue; it is less likely to observe this feature in leprosy or in hematogenous osteomyelitis periostitis [77,95]. Sinuous lacunae are described as smooth-walled porosities situated between the original cortical bone and the periosteal new bone formation [68]. Although sinuous lacunae are

not considered a feature used in the diagnosis of treponematosis, they can be used as useful criteria along with the other two histological features [3,96].

Von Hunnius et al. [3] performed paleohistological analyses on four treponematosis-affected individuals, discovered during archaeological excavations near the River Humber, England. Although microscopic preservation was poorer than that of the material presented in this study, osteons and interstitial lamellae as well as external and internal circumferential lamellae could be confidently identified in only two individuals. This limited preservation impeded the recognition of treponematosis-specific microstructural features described by Schultz [77]. Likewise, the study conducted by Assis et al. [97] reported that their histological assessment of an individual suspected of treponematosis was constrained by postmortem degradation.

The histological analysis conducted by Von Hunnius et al. [3] showed, in one individual, PNBF on the external surface on bone, described as "polsters", and composed of parallel bone lamellae. In two additional individuals, the PNBF resembling the structure reported by Schultz [77] was identified. Von Hunnius et al. [3] further noted that the newly formed tissue comprised both lamellar and primary bone and exhibited considerable morphological variability, being locally interrupted by crypts and fissures. In the present study, the PNBF on the external surface likewise displays a variable morphology, with polypoid and villous forms, particularly in the fibula of subject R30. A similarly variable periosteal morphology (sinuous and villous) was described by Assis et al. [97], based on the sectional contour of the fibula from an 18th century individual suspected of treponematosis. By contrast, in the humeri and femur of the R30 human skeleton and M40 human skeleton respectively, the newly formed tissue is more uniform, resembling a "polster-like" morphology, and exhibits fewer crypts than the fibula sample from the R30 individual. These formations are predominantly composed of lamellar bone, with focal areas of primary bone that may reflect the transition from an acute event to a chronic stage characterized by ongoing bone remodeling. This interpretation is further supported by the presence of osteons, for example, in the humerus of the R30 skeleton. Within the PNBF, remnants of vascular canals were observed, consistent with an inflammatory episode. Moreover, in the fibula of R30 skeleton, the layered development of the newly formed tissue suggests a recurrent periostitis. The identification of such episodic infectious events was also reported by Von Hunnius et al. [3].

Schultz's lamellar "grenzlinie" [77] was exceptionally well preserved in the samples from the M40 and R30 human skeletons. In contrast, in the R26 sample, this structure was only focally detectable and was absent in many microscopic fields. This pattern may be more consistent with osteitis than with periostitis, with the periosteal component—if present—likely representing an early stage. Van der Merwe et al. [98] likewise reported the absence of both "polsters" and "grenzlinie" in the tibia of an individual with treponematosis, describing cortical thickening with concomitant narrowing of the medullary canal; the cortex was traversed by numerous cavities, complicating the distinction between cortical and trabecular bone. Similarly, the paleohistological assessment by Assis et al. [97] of an individual suspected of treponematosis did not confirm "grenzlinie"-type structures, a result attributed in part to advanced postmortem histological alteration. Notably, interfaces separating cortical bone from newly formed tissue have been documented in other infectious conditions, including on the visceral surface of ribs from individuals diagnosed with tuberculosis in the first half of the 20th century [99] and in a fibular section from a clinically confirmed case of osteomyelitis [96].

In our study, the cortical bone showed marked osteoclastic activity, evidenced by abundant resorption lacunae and Howship lacunae. Osteolysis was most pronounced in the fibular sample from the R30 skeleton. Compared to the compact bone histoarchitecture

of the humeri belonging to the M40 and R30 skeletons, the compact tissue of the R26 skeleton is characterized by a more trabecular-like appearance, with fewer osteons and numerous resorption cavities, a pattern most consistent with osteoperiostitis. Except for the newly formed tissue observed in the humerus of subject R26, which locally exhibits features consistent with the "polsters" structure described by Von Hunnius et al. [3] and Schultz [77], the proliferative tissue in subjects M40 and R30 shows distinct morphologies, capturing transitional stages between acute inflammatory activity and a chronic course.

Histological assessment of the postcranial samples indicates a spectrum of tissue responses—including acute and chronic phases, hemorrhagic changes, proliferative (osteoblastic) activity, and destructive/osteolytic (osteoclastic) processes—that may be compatible with treponematosis. Nevertheless, the diagnostic specificity of these microstructural features (e.g., "polsters", "grenzlinie", and sinuous lacunae) for treponematosis remains uncertain, underscoring the need for additional comparative and methodologically standardized studies. In this regard, paleohistological analyses strengthen paleopathological reconstructions by complementing macroscopic observations and by providing refined information on disease stage (acute vs. chronic) and on the timing and extent of skeletal involvement at or near the time of death.

6. Conclusions

In the skeletal sample of the 15th–19th centuries discovered at the "Adormirea Maicii Domnului" Roman Catholic Cathedral of Iaşi, treponematosis was identified in three cases—two females aged between 30 and 40 years old and one male of 35–40 years old. The differential diagnosis is based on multiple methods of investigations—macroscopy (i.e., somatoscopy, radiography and computed tomography) as well as microscopy (i.e., histology).

The three individuals show multiple skull lesions as osteological symptoms of treponematosis and even acquired syphilis, representing different stages of *caries sicca* in the frontal and parietal bones. In the long bones (i.e., humeri, ulna, femora, tibiae, and fibula), cortical thickening and formation of new periosteal bone are reported. Particularly, the formation of new periosteal bone characterizes syphilis, and it may appear in the early stages, being prominent on the tibia, frontal bone, ribs, and sternum, although other bones may be involved. In the later stages of the disease, the skeletal lesions are due to the formation of gumma in bones. In the cranium, the bony tissues adjacent to gumma undergo necrosis, and it is absorbed; this process is termed *caries sicca*. Also, multiplex lytic lesions with irregular margins on the outer table and in the diploë were identified. The differential diagnosis applied to the identified lesions of the skeletons analyzed in this study leads to the conclusion that the treponematosis was present, probably acquired syphilis.

In the analyzed skeletons, probable treponematosis is not associated with other significant pathologies. However, there is a need to mention the identification of dental caries and dental calculus in the skeletons M40 and R26, wormian bones in M40, and the metopic suture in R26.

The histological investigation of postcranial inflammatory reactions in skeletons suspected of treponematosis recovered in Iași (15th–19th centuries) indicates acute and chronic, recurrent, osteoblastic, and osteoclastic episodes, which may follow different trajectories in different anatomical segments within the same individual. Good macroscopic and microscopic preservation of the skeletal material in an archaeological context enabled the description and identification of histological structural elements. The morphology of the periosteal new bone formation may serve as an indicator of recurrent treponemal infection. Newly formed tissue can display different structures and morphologies (homogeneous, polypoid, villous), depending on whether it reflects an acute (inflammatory) or chronic stage of treponemal infection.

Author Contributions: Conceptualization, V.-M.G. and O.-M.C.-P.; methodology, V.-M.G. and O.-M.C.-P.; validation, L.B. and A.-N.N.; investigation, V.-M.G., O.-M.C.-P., M.P. and A.-N.N.; resources, V.-M.G., O.-M.C.-P., A.-N.N. and L.B.; writing—original draft preparation, V.-M.G. and O.-M.C.-P.; writing—review and editing, L.B., V.-M.G. and O.-M.C.-P.; visualization, L.B., V.-M.G. and O.-M.C.-P.; supervision, L.B.; project administration, L.B.; funding acquisition, L.B. All authors have read and agreed to the published version of the manuscript.

Funding: This research was supported by a grant of the Ministry of Research, Innovation and Digitization, CNCS—UEFISCDI: project number PN-III-P4-PCE-2021-1180 within PNCDI III.

Data Availability Statement: Data are contained within the article.

Acknowledgments: We would like to express our gratitude to the archaeologists from the Romanian Academy, Iasi Branch, who provided us the skeletal material for study—Stela Cheptea and Bobi Apăvăloaei.

Conflicts of Interest: The authors declare no conflicts of interest.

References

1. Antal, G.M.; Lukehart, S.A.; Meheus, A.Z. The endemic treponematoses. *Microbes Infect.* **2002**, *4*, 83–94. [CrossRef] [PubMed]
2. Hackett, C.J. An introduction to diagnostic criteria of syphilis, treponarid and yaws (treponematoses) in dry bones, and some implications. *Virchows Arch.* **1975**, *368*, 229–241. [CrossRef]
3. Von Hunnius, T.E.; Roberts, C.A.; Boylston, A.; Saunders, S.R. Histological identification of syphilis in pre-Columbian England. *Am. J. Phys. Anthropol.* **2006**, *129*, 559–566. [CrossRef] [PubMed]
4. Salazar, J.C.; Bennett, N.J. Endemic treponematosis including yaws and other spirochaetes. In *Manson's Tropical Diseases*, 23rd ed.; Farrar, J., Hotez, P.J., Junghanss, T., Kang, G., Lalloo, D., White, N.J., Eds.; Elsevier: Philadelphia, PA, USA, 2014; pp. 421–432.e3.
5. Stamm, L.V. Pinta: Latin America's forgotten disease? *Am. J. Trop. Med. Hyg.* **2015**, *93*, 901–903. [CrossRef]
6. Walker, D.; Powers, N.; Connell, B.; Redfern, R. Evidence of Skeletal Treponematosis from the Medieval Burial Ground of St. Mary Spital, London, and Implications for the Origins of the Disease in Europe. *Am. J. Phys. Anthropol.* **2015**, *156*, 90–101. [CrossRef]
7. Kojima, N.; Klausner, J.D. An update on the global epidemiology of syphilis. *Curr. Epidemiol. Rep.* **2018**, *5*, 24–38. [CrossRef]
8. Mitjà, O.; Marks, M.; Konan, D.J.P.; Ayelo, G.; Gonzalez-Beiras, C.; Boua, B.; Asiedu, K. Global epidemiology of yaws: A systematic review. *Lancet Glob. Health* **2015**, *3*, e324–e331. [CrossRef]
9. Hackett, C.J. *Bone Lesions of Yaws in Uganda*; Blackwell: Oxford, UK, 1951.
10. Resnick, D.; Niwayama, G. Osteomyelitis, septic arthritis, and soft tissue infection: Organisms. In *Diagnosis of Bone and Joint Disorders*; Resnick, D., Ed.; W. B. Saunders: London, UK, 1995; pp. 2448–2559.
11. Giacani, L.; Lukehart, S.A. The endemic treponematoses. *Clin. Microbiol. Rev.* **2014**, *27*, 89–115. [CrossRef]
12. Hudson, E.H. Treponematosis and man's social evolution. *Am. Anthropol.* **1965**, *67*, 885–901. [CrossRef]
13. Baker, B.J.; Armelagos, G.J. The origin and antiquity of syphilis: Paleopathological diagnosis and interpretation. *Curr. Anthropol.* **1988**, *29*, 703–737. [CrossRef] [PubMed]
14. Harper, K.N.; Zuckerman, M.K.; Harper, M.L.; Kingston, J.D.; Armelagos, G.J. The origin and antiquity of syphilis revisited: An Appraisal of Old World pre-Columbian evidence for treponemal infection. *Am. J. Phys. Anthropol.* **2011**, *146*, 99–133. [CrossRef] [PubMed]
15. De Melo, F.L.; de Mello, J.C.; Fraga, A.M.; Nunes, K.; Eggers, S. Syphilis at the Crossroad of Phylogenetics and Paleopathology. *PLoS Neglected Trop. Dis.* **2010**, *4*, e575. [CrossRef]
16. Armelagos, G.J.; Zuckerman, M.K.; Harper, K.N. The Science Behind Pre-Columbian Evidence of Syphilis in Europe: Research by Documentary. *Evol. Anthropol.* **2012**, *21*, 50–57. [CrossRef]
17. Marinković, Z.; Đukić, S. The origin of syphilis—Still controversial? *Sanamed* **2012**, *7*, 127–130.
18. Knauf, S.; Liu, H.; Harper, K.N. Treponemal infection in nonhuman primates as possible reservoir for human yaws. *Emerg. Infect. Dis.* **2013**, *19*, 2058. [CrossRef]
19. Knauf, S.; Gogarten, J.F.; Schuenemann, V.J.; De Nys, H.M.; Düx, A.; Strouhal, M.; Calvignac-Spencer, S. Nonhuman primates across sub-Saharan Africa are infected with the yaws bacterium *Treponema pallidum* subsp. *pertenue*. *Emerg. Microbes Infect.* **2018**, *7*, 1–4. [CrossRef]
20. Hackett, C.J. *Diagnostic Criteria of Syphilis, Yaws and Treponarid (Treponematoses) and Some Other Diseases in Dry Bones (for Use in Osteoarcheology)*; Springer: Berlin/Heilderberg, Germany, 1976.
21. Aufderheide, A.C.; Rodríguez-Martín, C. *The Cambridge Encyclopedia of Human Paleopathology*; Cambridge University Press: New York, NY, USA, 1998.

22. Ortner, D.J.; Putschar, W.G.J. *Identification of Pathological Conditions in Human Skeletal Remains*; Smithsonian Institution Press: Washington, DC, USA, 1981.
23. Steinbock, R.T. *Paleopathological Diagnosis and Interpretation—Bone Diseases in Ancient Human Populations*; Charles Thomas Publishers: Springfield, IL, USA, 1976.
24. Ortner, D.J. *Identification of Pathological Conditions in Human Skeletal Remains*; Academic Press: London, UK, 2003.
25. Vargová, L.; Vymazalová, K.; Horáčková, L. A brief history of syphilis in the Czech Lands. *Archaeol. Anthropol. Sci.* **2019**, *11*, 521–530. [CrossRef]
26. Crosby, A.W. The early history of syphilis: A reappraisal. *Am. Anthropol.* **1969**, *71*, 218–227. [CrossRef]
27. Goff, C.W. Syphilis. In *Diseases in Antiquity*; Brothwell, D., Sandison, A.T., Eds.; Charles C. Thomas: Springfield, IL, USA, 1967; pp. 279–293.
28. Pusey, W.A. *The History and Epidemiology of Syphilis*; Charles C. Thomas: Springfield, IL, USA, 1933.
29. Cockburn, T.A. The origin of the treponematoses. *Bull. WHO* **1961**, *24*, 221–228. [PubMed]
30. Hackett, C.J. The human treponematoses. In *Diseases in Antiquity*; Brothwell, D., Sandison, A.T., Eds.; Charles, C. Thomas: Springfield, IL, USA, 1967; pp. 152–169.
31. Holcomb, R.C. *Who Gave the World Syphilis? The Haitian Myth*; Froben Press: New York, NY, USA, 1937.
32. Hudson, E.H. Christopher Columbus and the history of syphilis. *Acta Trop.* **1968**, *25*, 1–16. [PubMed]
33. Roberts, C.A.; Manchester, K. *The Archaeology of Disease*; Cornell University Press: New York, NY, USA, 1995.
34. Ortner, D.J.; Tuross, N.; Stix, A.I. New approaches to the study of disease in archeological New World populations. *Hum. Biol.* **1992**, *64*, 337–360.
35. Centurion-Lara, A.; Castro, C.; Castillo, R.; Shaffer, J.M.; Van Voorhis, W.C.; Lukehart, S.A. The flanking region sequences of the 15-kDa lipoprotein gene differentiate pathogenic treponemes. *J. Infect. Dis.* **1998**, *177*, 1036–1040. [CrossRef]
36. Gray, R.; Mulligan, C.; Molini, B.; Sun, E.; Giacani, L.; Godornes, C.; Kitchen, A.; Lukehart, S.; Centurion-Lara, A. Molecular evolution of the tprC, D, I, K, G, and J genes in the pathogenic genus Treponema. *Mol. Biol. Evol.* **2006**, *23*, 2220–2233. [CrossRef]
37. Harper, K.N.; Ocampo, P.S.; Steiner, B.M.; George, R.W.; Silverman, M.S.; Bolotin, S.; Pillay, A.; Saunders, N.J.; Armelagos, G.J. On the origin of the treponematoses: A phylogenetic approach. *PLoS Neglected Trop. Dis.* **2008**, *2*, e148. [CrossRef] [PubMed]
38. Rissech, C.; Roberts, C.; Tomás-Batlle, X.; Tomás-Gimeno, X.; Fuller, B.; Fernandez, P.L.; Botella, M. A roman skeleton with possible treponematosis in the north-east of the Iberian Peninsula: A morphological and radiological study. *Int. J. Osteoarchaeol.* **2013**, *23*, 651–663. [CrossRef]
39. Bouwman, A.S.; Brown, T.A. The limits of biomolecular palaeopathology: Ancient DNA cannot be used to study venereal syphilis. *J. Archaeol. Sci.* **2005**, *32*, 703–713. [CrossRef]
40. Kolman, C.J.; Centurion-Lara, A.; Lukehart, S.A.; Owsley, D.W.; Tuross, N. Identification of Treponema pallidum subspecies pallidum in a 200-year-old skeletal specimen. *J. Infect. Dis.* **1999**, *180*, 2060–2063. [CrossRef] [PubMed]
41. Schuenemann, V.J.; Lankapalli, A.K.; Barquera, R.; Nelson, E.A.; Hernández, D.I.; Alonzo, V.A.; Bos, K.I.; Morfín, L.M.; Herbig, A.; Krause, J. Historic Treponema pallidum genomes from colonial Mexico retrieved from archaeological remains. *PLoS Neglected Trop. Dis.* **2018**, *12*, e0006447. [CrossRef]
42. Giffin, K.L.; Lankapalli, A.K.; Sabin, S.; Spyrou, M.A.; Posth, C.; Kozakaitė, J.; Friedrich, R.; Miliauskienė, Ž.; Jankauskas, R.; Herbig, A.; et al. A treponemal genome from an historic plague victim supports a recent emergence of yaws and its presence in 15th century Europe. *Sci. Rep.* **2020**, *10*, 9499. [CrossRef]
43. Majander, K.; Pfrengle, S.; Kocher, A.; Neukamm, J.; du Plessis, L.; Pla-Díaz, M.; Arora, N.; Akgül, G.; Salo, K.; Schats, R.; et al. Ancient bacterial genomes reveal a high diversity of Treponema pallidum strains in Early Modern Europe. *Curr. Biol.* **2020**, *30*, 3788–3803.e10. [CrossRef] [PubMed]
44. Arora, N.; Schuenemann, V.J.; Jäger, G.; Peltzer, A.; Seitz, A.; Herbig, A.; Strouhal, M.; Grillová, L.; Sánchez-Busó, L.; Kühnert, D.; et al. Origin of modern syphilis and emergence of a pandemic Treponema pallidum cluster. *Nat. Microbiol.* **2016**, *2*, 16245. [CrossRef]
45. Barquera, R.; Sitter, T.L.; Kirkpatrick, C.L.; Ramirez, D.A.; Arthu Kocher, A.; Spyrou, M.A.; Couoh, L.R.; Talavera-González, J.A.; Castro, M.; von Hunnius, T.; et al. Ancient genomes reveal a deep history of Treponema pallidum in the Americas. *Nature* **2025**, *640*, 186–193. [CrossRef]
46. Groza, V.-M.; Popovici, M.; Bejenaru, L.; Petraru, O.-M. Preliminary study of human skeleton with syphilis discovered in the postmedieval city of Iași (Romania). *RAASI* **2020**, *2*, 319–328.
47. Djurić-Srejić, M.; Roberts, C. Palaeopathological evidence of infectious disease in skeletal populations from later medieval Serbia. *Int. J. Osteoarchaeol.* **2001**, *11*, 311–320. [CrossRef]
48. Gaul, J.S.; Grossschmidt, K. A probable case of congenital syphilis from 18th century Vienna. *Int. J. Paleopathol.* **2014**, *6*, 34–43. [CrossRef]
49. Gladykowska-Rzeczycka, J.J.; Kwiatkowska, B.; Nowakowski, D.; Trnka, J. Treponematosis in a 14th century skeleton from Wroclaw, Poland. *J. Paleopathol.* **2003**, *15*, 187–193.

50. Ősz, B. Paleopathological investigations of the skeletal material of Szeged-Vár, Hungary. *Acta Biol. Szeged.* **2006**, *50*, 167.
51. Pietrobelli, A.; Mariotti, V.; Fusari, S.; Gasparini, A.; Bettuzzi, M.; Morigi, M.P.; Belcastro, M.G. Syphilis in an Italian medieval jewish community: A bioarchaeological and cultural perspective. *Int. J. Paleopathol.* **2020**, *30*, 85–97. [CrossRef] [PubMed]
52. Roberts, C.A.; Millard, A.R.; Nowell, G.M.; Gröcke, D.R.; Macpherson, C.G.; Pearson, D.G.; Evans, D.H. Isotopic tracing of the impact of mobility on infectious disease: The origin of people with treponematosis buried in hull, England, in the late medieval period. *Am. J. Phys. Anthropol.* **2013**, *150*, 273–285. [CrossRef]
53. Šlaus, M.; Novak, M. A Case of Venereal Syphilis in the Modern Age Horizon of Graves near the Church of St. Lawrence in Crkvari. *Pril. Inst. Arheol. Zagrebu.* **2007**, *24*, 503–510.
54. Tomczyk, J.; Mańkowska-Pliszka, H.; Palczewski, P.; Olczak-Kowalczyk, D. Congenital syphilis in the skeleton of a child from Poland (Radom, 18th–19th century AD). *Anthropol. Rev.* **2015**, *8*, 79–90. [CrossRef]
55. Radu, C.; Andreica, L.; Constantinescu, M.; Soficaru, A. Multiple Cases with Probable Treponemal Infection from 16th to 19th Centuries Romania. *Int. J. Osteoarchaeol.* **2016**, *26*, 563–573. [CrossRef]
56. Cihodaru, C.; Cristian, V.; Dinu, M.; Neamţu, V.; Petrescu-Dîmboviţa, M.; Platon, G.; Rusu, D.; Timofte, M. *Istoria Oraşului Iaşi*; Junimea: Iaşi, Romania, 1980.
57. Cloşcă, C. *Iaşul*; Ştef: Iaşi, Romania, 2008.
58. Caproșu, I. *Documente Privitoare la Istoria Orașului Iași*; Dosoftei: Iași, Romania, 2001.
59. Apăvăloaei, B. Amenajarea Râului Bahlui în Secolul al XVII-lea la Iaşi. *Carpica* **2010**, *39*, 141–153.
60. Cheptea, S. Biserica romano-catolică "Adormirea Maicii Domnului" din Iaşi. *Eur. XXI* **1995**, *3–4*, 277–288.
61. Chelcu, M. Orăşenii din Iaşi în secolul XVII-solidarităţi şi diferenţe. *AIIGB* **2010**, *49*, 39–47.
62. Murgescu, B.; Bonciu, F. Consideraţii asupra abordării mondiale a proceselor istorico-economice. *AIIX* **1993**, *30*, 523–547.
63. Samarian, P.G. *Medicina şi Farmacia în Trecutul Românesc*; II 1775-1834; Tipografia Cultura: Bucharest, Romania, 1938.
64. Groza, V.-M.; Miu, G.; Simalcsik, A.; Simalcsik, R. Reconstruction of the demographic profile and the longevity of the population inhabiting the city of Iaşi during the late middle ages and the early modern period (15th–19th centuries). *An. St. Univ. "Al. I. Cuza" Iaşi* **2013**, *LIX*, 115–128.
65. Bogdan, N.A. *Orasul Iasi. Monografie Istorica si Sociala Ilustrata*; Editura Tehnopres: Iaşi, Romania, 2004.
66. Bello, S.M.; Thomann, A.; Signoli, M.; Dutour, O.; Andrews, P. Age and sex bias in the reconstruction of past population structures. *Am. J. Phys. Anthropol.* **2006**, *129*, 24–38. [CrossRef]
67. Waldron, T. *Palaeopathology*; Cambridge University Press: Cambridge, UK, 2008.
68. Cooke, K.M. Palaeohistopathology of Treponematosis in Human Bone. Ph.D. Thesis, The Australian National University, Canberra, Australia, 2024.
69. Squires, K.; Booth, T.; Roberts, C.A. The ethics of sampling human skeletal remains for destructive analyses. In *Ethical Approaches to Human Remains: A Global Challenge in Bioarchaeology and Forensic Anthropology*; Squires, K., Errickson, D., Márquez-Grant, N., Eds.; Springer: Berlin/Heilderberg, Germany, 2020; pp. 265–297.
70. García-Donas, J.G.; Dalton, A.; Chaplin, I.; Kranioti, E. A revised method for the preparation of dry bone samples used in histological examination: Five simple steps. *HOMO* **2017**, *68*, 283–288. [CrossRef]
71. Heck, C.T.; Volkmann, G.; Woodward, H.N. Polyester or epoxy: Assessing embedding product efficacy in paleohistological methods. *PeerJ* **2020**, *8*, e10495. [CrossRef]
72. Hedges, R.E.; Millard, A.R.; Pike, A. Measurements and relationships of diagenetic alteration of bone from three archaeological sites. *J. Archaeol. Sci.* **1995**, *22*, 201–209. [CrossRef]
73. Hollund, H.I.; Blank, M.; Sjögren, K.-G. Dead and buried? Variation in post-mortem histories revealed through histotaphonomic characterisation of human bone from megalithic graves in Sweden. *PLoS ONE* **2018**, *13*, e0204662. [CrossRef] [PubMed]
74. Thompson, J.E.; Panella, S.; Booth, T.J.; Soncin, S.; Rajkovaca, T.; Belcastro, M.G.; Isetti, E.; Mariotti, V.; Muntoni, I.M.; Radina, F. Histotaphonomic analysis of bone bioerosion reveals a regional framework of diverse deathways in the Neolithic of Southeast Italy. *PLoS ONE* **2024**, *19*, e0304058. [CrossRef]
75. Papakonstantinou, N.; Booth, T.; Triantaphyllou, S. Human remains under the microscope of funerary taphonomy: Investigating the histological biography of the decaying body in the prehistoric Aegean. *J. Archaeol. Sci. Rep.* **2020**, *34*, 102654. [CrossRef]
76. Turner-Walker, G. Light at the end of the tunnels? The origins of microbial bioerosion in mineralised collagen. *Palaeogeogr. Palaeoclimatol. Palaeoecol.* **2019**, *529*, 24–38. [CrossRef]
77. Schultz, M. Paleohistopathology of bone: A new approach to the study of ancient diseases. *Am. J. Phys. Anthropol.* **2001**, *116*, 106–147. [CrossRef]
78. Ciorpac-Petraru, O.-M. *Dincolo de Lentila Microscopului. Analiza unor Resturi Umane Vechi Descoperite în Situri Arheologice din Nord-Estul României*; Editura MEGA: Cluj-Napoca, Romania, 2025.
79. Hernandez, M.; Hudson, M.J. Diagnosis and evaluation of causative factors for the presence of endemic treponemal disease in a Japanese sub-tropical island population from the Tokugawa period. *Int. J. Paleopathol.* **2015**, *10*, 16–25. [CrossRef]

80. Ortner, D.J. Differential diagnosis of skeletal lesions in infectious disease. In *Advances in Human Paleopathology*; Pinhasi, R., Mays, S., Eds.; John Wiley & Sons, Ltd.: West Sussex, UK, 2008; pp. 191–214.
81. Gennari, L.; Rendina, D.; Falchetti, A.; Merlotti, D. Paget's disease of bone. *Calcif. Tissue Int.* **2019**, *104*, 483–500. [CrossRef]
82. Ramos Van Raap, M.A.; Scabuzzo, C. A case of non-venereal treponematosis in a pre-Hispanic adult from north-eastern Argentina. *Int. J. Osteoarchaeol.* **2018**, *28*, 757–765. [CrossRef]
83. Roberts, C.A.; Buikstra, J.E. Bacterial infections. In *Ortner's Identification of Pathological Conditions in Human Skeletal Remains*; Buikstra, J.E., Ed.; Academic Press: Amsterdam, The Netherlands, 2019; pp. 321–439.
84. Kharlamova, N.; Ogarkov, O.; Berdnikov, I.; Berdnikova, N.; Galeev, R.; Mokrousov, I. Bioarchaeological and molecular evidence of tuberculosis in human skeletal remains from 18th–19th century orthodox cemeteries in Irkutsk, Eastern Siberia. *Tuberculosis* **2023**, *143*, 102368. [CrossRef]
85. Marais, S.; Roos, I.; Mitha, A.; Mabusha, S.J.; Patel, V.; Bhigjee, A.I. Spinal tuberculosis: Clinicoradiological findings in 274 patients. *Clin. Infect. Dis.* **2018**, *67*, 89–98. [CrossRef] [PubMed]
86. Sparacello, V.S.; Roberts, C.A.; Kerudin, A.; Müller, R. A 6500-year-old Middle Neolithic child from Pollera Cave (Liguria, Italy) with probable multifocal osteoarticular tuberculosis. *Int. J. Paleopathol.* **2017**, *17*, 67–74. [CrossRef]
87. Papa, V.; Varotto, E.; Vaccarezza, M.; Galassi, F.M. Morphologic and Clinical Aspects of Pott Disease in Ancient Human Remains: A Scoping Review. *Spine* **2025**, *50*, E56–E69. [CrossRef]
88. Marden, K.; Ortner, D.J. A case of treponematosis from pre-Columbian Chaco Canyon, New Mexico. *Int. J. Osteoarchaeol.* **2011**, *21*, 19–31. [CrossRef]
89. Powell, M.L.; Cook, D.C. Treponematosis: Inquiries into the nature of a protean disease. In *The Myth of Syphilis: The Natural History of Treponematosis in North America*; Powell, M.L., Cook, D.C., Eds.; University Press of Florida: Gainsville, FL, USA, 2005; pp. 9–62.
90. Morand, J.J.; Simon, F.; Garnotel, E.; Mahe, A.; Clity, E.; Morlain, B. Overview of endemic treponematoses. *Med. Trop.* **2006**, *66*, 15–20.
91. Cook, D.C.; Powell, M.L. Treponematosis: Past, present, and future. In *A Companion to Paleopathology*; Grauer, A., Ed.; Blackwell: West Sussex, UK, 2012; pp. 472–491.
92. Musher, D.M.; Baughn, R.E. Syphilis. In *Infectious Diseases*; Gorbach, S.L., Bartlett, J.G., Blacklow, N.R., Eds.; W.B. Saunders Company: Philadelphia, PA, USA, 1998; pp. 980–986.
93. Schultz, M. Comparative histopathology of syphilitic lesions in prehistoric and historic human bones. In *L'Origine de la Syphilis en Europe Avant ou Apres*; Dutour, O., Pálfi, G., Bérato, J., Brun, J.-P., Eds.; Ed. Errance: Toulon, France, 1994; Volume 1493, pp. 63–67.
94. Mikita, G.; Lizoń, M.J.; Gąsiorowska, J.; Hanypsiak, M.M.; Falana, J.; Mazurek, M.; Pioterek, O.W.; Wolak, K.; Grzelak, J.; Domagała, D. Diagnostic Methods Used in Detecting Syphilis in Paleopathological Research—A Literature Review. *Diagnostics* **2025**, *15*, 1116. [CrossRef]
95. Schultz, S.T.H.; Schultz, M. Identification of typical marker proteins of Treponema pallidum in compact human bone using morphological and biochemical techniques. *Sci. Rep.* **2025**, *15*, 28743. [CrossRef]
96. Weston, D.A. Brief communication: Paleohistopathological analysis of pathology museum specimens: Can periosteal reaction microstructure explain lesion etiology? *Am. J. Phys. Anthr.* **2009**, *140*, 186–193. [CrossRef]
97. Assis, S.; Casimiro, S.; Alves Cardoso, F. A possible case of acquired syphilis at the former Royal Hospital of All-Saints (RHAS) in Lisbon, Portugal (18th century). *Anthropol. Anz.* **2015**, *72*, 427–449. [CrossRef]
98. Van der Merwe, A.; Maat, G.; Steyn, M. Ossified haematomas and infectious bone changes on the anterior tibia: Histomorphological features as an aid for accurate diagnosis. *Int. J. Osteoarchaeol.* **2010**, *20*, 227–239. [CrossRef]
99. Assis, S.; Keenleyside, A. The macroscopic and histomorphological properties of periosteal rib lesions and its relation with disease duration: Evidence from the Luis Lopes Skeletal Collection (Lisbon, Portugal). *J. Anat.* **2019**, *234*, 480–501. [CrossRef]

Disclaimer/Publisher's Note: The statements, opinions and data contained in all publications are solely those of the individual author(s) and contributor(s) and not of MDPI and/or the editor(s). MDPI and/or the editor(s) disclaim responsibility for any injury to people or property resulting from any ideas, methods, instructions or products referred to in the content.